Joint Optimization of Park-and-Ride Facility Locations and Alternate Traffic Restriction Scheme under Equilibrium Flows

Guangming Xu[a], Yanqin Chen[a], Wei Liu[b,*]

[a] *School of Traffic and Transportation Engineering, Central South University, Changsha, Hunan 410075, China*

[b] *Department of Aeronautical and Aviation Engineering, The Hong Kong Polytechnic University, Hong Kong, China*

[*] *Corresponding author: wei.w.liu@polyu.edu.hk (W. Liu)*

Abstract

Alternate traffic restriction (ATR) or road space rationing schemes manage traffic congestion by prohibiting a proportion of cars from entering a predetermined ATR area during designated time periods or days. Under the ATR scheme, Park-and-Ride (P&R) often becomes more popular as travelers are able to take advantage of driving on non-restricted roads while they can park their cars at P&R facilities and do not need to drive into the predetermined ATR area. This paper proposes a joint optimization model of P&R facility locations and the ATR scheme, which optimally designs the ATR areas, the proportion of private cars to be restricted, and the P&R facility locations. In particular, a multi-objective bi-level model is established. The upper-level model minimizes the total travel cost, minimizes the total emission cost, and maximizes consumer surplus. The lower-level model characterizes the user equilibrium of travel mode choices (i.e., private car mode, public transport mode, and P&R mode) and the route choices. The non-dominated sorting genetic algorithm (NSGA-II) is adapted to solve the proposed multi-objective bi-level model, where a gradient project algorithm is proposed for solving the lower-level user equilibrium with both mode choices and route choices. Numerical studies are conducted to test and illustrate the applicability of the model and algorithms.

Keywords: Park-and-ride location; Alternate traffic restriction; Multi-objective optimization; Bi-level programming

1. Introduction

Under increasing car ownership and usage, traffic congestion and vehicular emission have become increasingly severe. In order to alleviate traffic congestion and reduce urban vehicular emission, many management strategies have been proposed, such as congestion pricing (Yang and Huang, 2005; Lindsey, 2010; Cheng et al., 2019; Han et al., 2021); parking charges (Arnott et al., 1991; Zhang et al., 2008; Liu and Geroliminis, 2016); tradable travel credits (Yang and Wang, 2011; Wang et al., 2012; Wu et al., 2012), and alternate traffic restriction or road space rationing (Daganzo, 1995; Liu et al., 2014). While congestion pricing has only been implemented in a few cities due to strong public objection, the alternate traffic restriction or road space rationing has been implemented with less objections in many cities worldwide. For example, Beijing has implemented a spatial rationing scheme to restrict driving based on the last digits or letters of vehicle license plates since Beijing hosted the 2008 Summer Olympics. Several studies have examined the efficiency of the license-plate-based traffic rationing schemes (e.g., Han et al., 2010), and some further modified the rationing schemes to improve its effectiveness (Nie, 2017). By June 2016, there are in total 12 cities in China that have adopted similar driving restriction schemes.[1]

Alternate traffic restriction (ATR), which is alternatively termed as "road space rationing" (Daganzo, 1995) or "vehicle restriction" (Grange and Troncoso, 2011), prohibits a proportion of vehicles from entering designated ATR areas during designated time periods or days. Travelers have to use other travel alternatives when their vehicles are restricted. ATR is considered an effective strategy to control the total road traffic, as evidenced by practices in, e.g., Beijing. Daganzo (1995) examined the potential of the "hybrid between rationing and pricing" to be Pareto-improving, where a certain proportion of vehicles (travelers) should pay a toll if they choose to drive on certain days. Such a hybrid scheme is more flexible than the pure ATR scheme. Nakamura and Kockelman (2002) evaluated the hybrid scheme proposed by Daganzo (1995) in the San Francisco Bay Bridge case. Later, Daganzo and Garcia (2011) further extended Daganzo (1995) to the time-dependent case. Recently, Song et al. (2013) proposed models to find the Pareto-improving hybrid scheme of rationing and pricing in general road networks. Shi et al., (2014) optimized the ATR scheme in order to maximize consumer surplus, where three modes, i.e., private car, public transport and park-and-ride (P&R), are all considered. However, the locations of P&R facilities were taken as exogenous input in Shi et al., (2014). Liu et al. (2014) examined the rationing and pricing scheme in a linear traffic corridor, where optimal P&R facility locations along the corridor can be identified. This study further examines the joint optimization of P&R facility locations and alternate traffic restriction scheme in a general network with elastic demand and multimodality, where the

[1] The great crawl - The Chinese love their cars but do not want to pay more for driving them, available at https://www.economist.com/china/2016/06/16/the-great-crawl?frsc=dg%7Ca, accessed on June 01, 2021.

optimal P&R facility locations and ATR scheme are interdependent and together govern users' travel choices. Moreover, this study considers that there are three objectives to be optimized simultaneously when designing the P&R facility locations and ATR scheme, i.e., to minimize total travel cost, minimize the total emission cost, and maximize consumer surplus.

Travelers choosing P&R mode can first park their cars in the P&R facilities and then transfer to the public transport system (such as bus, subway, light rail systems) to reach their final destinations. P&R mode has been recognized as an effective way to alleviate traffic congestion, reduce the mileage of private cars, increase the utilization rate of public transport systems, and reduce vehicular emission (Wang et al., 2004; Liu et al., 2009; Liu and Meng, 2014; Liu et al., 2017). A series of policy-oriented empirical studies discussed many aspects of P&R mode. For instance, Dijk and Montalvo (2011) summarized the policy frames of P&R mode in European cities. Duncan and Christensen (2013) indicated that the station area characteristics were significant predictors of the light-rail based P&R in the US.

Wang et al. (2004) and Liu et al. (2009) developed traffic equilibrium models and examined the effect of P&R facilities and pricing on travel choice behaviours in a linear monocentric city. Farhan and Murray (2008) presented a multi-objective spatial optimization model for siting park-and-ride facilities, where they aim to cover as much potential demand as possible, locate park-and-ride facilities as close as possible to major roadways, and sit such facilities in the context of an existing system. Aros-Vera et al. (2013) studied P&R facility's location problems using logit model, where travelers could either select transfer (P&R) facilities or choose a car travel. Pineda et al. (2016) proposed a multimodal stochastic equilibrium model with P&R facilities in order to characterize route choices of travelers. Liu et al. (2017) proposed an adaptive and time-dependent pricing strategy in a multimodal network with P&R facilities located at the boundary of city center. Song et al. (2017) proposed an integrated planning model for P&R facilities and public transport service in the multimodal transport system. Liu et al. (2018) further proposed the concept of "Remote Park-and-Ride", where the parking facility locates in a suburban with relatively low land value and dedicated bus line connects the parking with a nearby train stop. More recently, Jakob and Menendez (2020) analyzed how introducing parking pricing inside a network, or a congestion toll combined with a park and ride (P&R) scheme can affect the drivers' decision between entering the network by car or using P&R. However, all of the aforementioned studies mainly focused on the P&R facilities and network traffic pattern, and did not consider the ATR scheme and its optimal integration with P&R facility location decisions.

In this paper, a multi-objective bi-level model is formulated to jointly optimize the ATR scheme and locations of P&R facilities, where we minimize the total travel cost, minimize the total emission cost, and maximize the consumer surplus. In the bi-level model the upper-level model

is to optimally design the restriction area (for the ATR scheme), the restricted ratio (for the ATR scheme), and the P&R facility location. The lower-level model considers the multimodal equilibrium traffic pattern, including private car, public transport, and P&R mode, where we have multi-class users (those being restricted and not restricted users for some areas or road links under the ATR scheme). A non-dominated sorting genetic algorithm (NSGA-II) is adopted to solve the proposed multi-objective bi-level model, where a gradient projection algorithm is proposed for solving the lower-level network equilibrium model. Numerical studies are further conducted to illustrate the applicability of the proposed optimization method for P&R facility locations and ATR scheme.

This study contributes to the literature as follows. (i) This study is the first to propose the multi-objective bi-level model for joint optimizing P&R facility locations and ATR scheme under elastic demand. The effectiveness and applicability of the proposed method is demonstrated with both toy network and real-world network examples. (ii) This study considers the trade-off among multiple objectives (trave cost, emission cost, and consumer surplus), where NSGA-II is used to solve the multi-objective model (upper-level in the bi-level model), and a gradient project algorithm is used to solve the lower-level user equilibrium with both mode choices and route choices. The solution approach also ensures that the restriction area in the ATR scheme is a single connected area. This study adds additional examples to the literature on how to use these technologies to solve complex bi-level optimization problem in transportation.

The rest of the paper is organized as follows. Section 2 introduces the multimodal network equilibrium model (lower-level problem) under given P&R facility locations and ATR scheme. Section 3 introduces the upper-level multi-objective model that concerns the total travel cost, the total emission cost, and the consumer surplus. Section 4 presents the non-dominated sorting genetic algorithm to solve the model. Section 5 is the numerical study. Section 6 concludes.

2. User equilibrium under given P&R facility location and ATR scheme

This section formulates the Logit-model based multimodal traffic equilibrium (both mode choices and route choices) under given P&R facilities and ATR scheme. The equilibrium formulation follows that in Shi et al. (2014). We first list the notations, and then introduce the basic considerations for the multimodal traffic equilibrium. Furthermore, based on the route cost formulations, we present the multi-class user equilibrium model for the multimodal network. The “multi-class” here refers to users restricted by the ATR scheme (not allowed to drive into a designed area) and users not restricted by the ATR scheme (allowed to drive into any road links), which are referred to as “restricted users” and “non-restricted users” hereinafter. Note that the same users can be “restricted users” (to drive into a designed area) on certain days

and "non-restricted users" on other days. The proportion of days a traveler is restricted should be equal to the proportion of travelers that are restricted on a given day, i.e., travelers are restricted on an evenly rotating basis. We focus on the traffic equilibrium for a given day. In practice the restriction ratio or proportion can be approximately achieved by restricting vehicles based on their vehicle plate numbers (e.g., based on the last digits of the plate number), where such a strategy is used in cities such as Beijing.

We summarize the main notations below.

Sets and indices	
G	the network where $G = (V, A^{\mathrm{au}}, A^{\mathrm{tr}})$
V	the set of nodes
A^{au}	the set of private car links
A^{tr}	the set of public transport system links
RS	the set of OD pairs
Q_{rs}	the travel demand for OD pair (r, s)
T	the set of available P&R facility location
T_0	the set of candidate P&R transfer facility
N^{au}	the restricted private car users
R^{au}	the non-restricted private car users
N^{pr}	the restricted P&R users
R^{pr}	the non-restricted P&R users
Variables	
$\omega_{rs}^{\mathrm{au}}$	the mean route cost of private car users for OD pair (r, s)
$\omega_{rs}^{\mathrm{tr}}$	the mean route cost of public transport users for OD pair
$\omega_{rs}^{\mathrm{pr}}$	the mean route cost of P&R users for OD pair (r, s)
u_{rs}^{au}	minimum route cost for private cars from OD pair $(r, s) \in RS$
$\tilde{u}_{rs}^{\mathrm{au}}$	minimum route cost for private cars from OD pair $(r, s) \in RS^{\mathrm{au}}$
u_{rs}^{tr}	the travel time of public transport for OD pair (r, s)
$\tilde{u}_{rs}^{pt}$	minimum route cost for restricted private car users who transfer to P&R or public transport with a new route between OD pair $(r, s) \in RS \backslash RS^{\mathrm{au}}$
u_{rs}^{pr}	minimum route cost for P&R users between OD pair $(r, s) \in RS$
$\tilde{u}_{rs}^{\mathrm{pr}}$	minimum route cost for restricted P&R users who s transfer to public transport with a new route between OD pair $(r, s) \in RS^{\mathrm{au}}$
q_{rs}^{au}	the private car demand for OD pair (r, s)
q_{rs}^{tr}	the public transport demand for OD pair (r, s)
q_{rs}^{pr}	the P&R demand for OD pair (r, s)
x_a	the flow of link $a \in A^{\mathrm{au}}$
t_a	the travel time for private cars of link $a, a \in A$
c_{rsp}^{au}	route cost for private cars on route $p \in P_{rs}^{\mathrm{au}}, (r, s) \in RS$
$\tilde{c}_{rsp}^{\mathrm{au}}$	route cost for private cars on route $p \in \tilde{P}_{rs}^{\mathrm{au}}, (r, s) \in RS^{\mathrm{au}}$
$\tilde{c}_{rsp}^{\mathrm{au}}$	route cost for private cars on route $p \in \bigcup_{t \in T \cup \{r\}} \tilde{P}_{rst}^{\mathrm{pr}}, (r, s) \in RS \backslash RS^{\mathrm{au}}$

c_{rsp}^{pr}	route cost for P&R on route $p \in P_{rst}^{\mathrm{pr}}, (r,s) \in RS$
$\tilde{c}_{rsp}^{\mathrm{pr}}$	route cost for P&R on route $p \in \tilde{P}_{rst}^{\mathrm{pr}}, (r,s) \in RS^{\mathrm{pr}}$
f_{rsp}^{au}	the flow of private cars on route $p, p \in P_{rs}^{\mathrm{au}}, (r,s) \in RS$
$\tilde{f}_{rsp}^{\mathrm{au}}$	the flow of private cars on route $p, p \in \tilde{P}_{rs}^{\mathrm{au}}, (r,s) \in RS^{\mathrm{au}}$
$\tilde{f}_{rsp}^{\mathrm{au}}$	the flow of private cars on route $p, p \in \bigcup_{t \in T \cup \{r\}} \tilde{P}_{rst}^{\mathrm{pr}}, (r,s) \in RS \backslash RS^{\mathrm{au}}$
f_{rsp}^{pr}	the flow of P&R on route p, $p \in P_{rst}^{\mathrm{pr}}, (r,s) \in RS$
$\tilde{f}_{rsp}^{\mathrm{pr}}$	the flow of P&R on route p, $p \in \tilde{P}_{rst}^{\mathrm{pr}}, (r,s) \in RS^{\mathrm{pr}}$
D	the restriction area under the ATR scheme
γ	the restriction ratio (proportion of users being restricted to enter the restriction area)
t	the node of P&R facility location
Parameters	
α_1^{tr}	the cost parameters
β	the parameter in the Logit model
α, m	the link travel time function parameters
t_{a0}	the free flow travel time of link a
c_a	the capacity of link a

Given the P&R facilities, travelers have three available travel modes, i.e., private car, public transport, and P&R mode. Under the ATR scheme, a proportion of travelers are prohibited to drive into designated ATR areas (this proportion might be referred to as "restriction ratio" hereinafter, which should be optimized). Non-restricted users and restricted users have different route sets. We consider that all users can always take public transport to reach their destination. For those choosing private car and P&R, if they are restricted users, they cannot drive on designated road links. Observe that users choosing P&R mode might be restricted as they still need to drive to the P&R transfer site in order to connect to public transport and this part of driving has to avoid the restriction area under the ATR scheme. For some OD pairs, all driving routes (for restricted users) might be blocked due to the ATR scheme, the restricted users then have to transfer to public transport or P&R mode (i.e., "private car users" indeed become public transport or P&R users, this will be modeled endogenously in the network equilibrium below). Different designs of ATR areas/districts, restriction ratios (proportion of restricted users), and P&R facility locations can yield different user travel choices and network traffic patterns.

Consider a network denoted by $G = (V, A^{\mathrm{au}}, A^{\mathrm{tr}})$, where V, A^{au} and A^{tr} are the set of nodes, the link sets for private cars and public transport, respectively (note that we let 'au' indicate private car mode, 'pr' indicate P&R mode, and 'tr' indicate public transport mode). The set of OD pairs is denoted as RS. The potential travel demand is denoted by $\bar{Q}_{rs} > 0$ for each OD pair $(r,s) \in RS$. The (realized) travel demand for OD pair (r,s) is given by:

$$Q_{rs} = \bar{Q}_{rs} \exp(-\eta \omega_{rs}) \qquad (r,s) \in RS \qquad (1)$$

where η is a positive coefficient in the elastic demand function that reflects how sensitive the demand is with respect to the cost, and ω_{rs} is the expected minimum travel cost for travelers between OD pair (r, s). When the value of η is larger, the demand decreases more sharply with respect to the travel cost. Among the total demand, travelers choosing private cars and P&R can be grouped into restricted users N^{au} and N^{pr} and non-restricted users R^{au} and R^{pr}, respectively.

In line with the Logit-model for mode choice that will be formulated in Eqs. (3)-(5), the expected minimum travel cost (Fernández et al, 2003; Ho et al., 2006) for OD pair (r, s) can be formulated as follows:

$$\omega_{rs} = -\frac{1}{\beta}\ln\left[\exp\{-\beta\omega_{rs}^{\mathrm{au}}\} + \exp\{-\beta\omega_{rs}^{\mathrm{tr}}\} + \exp\{-\beta\omega_{rs}^{\mathrm{pr}}\}\right] \qquad (r,s) \in RS \qquad (2)$$

where β is a positive coefficient in the Logit-model for mode choice given in Eqs. (3)-(5), and for OD pair (r, s), $\omega_{rs}^{\mathrm{au}}$ is the mean route cost of private car mode, $\omega_{rs}^{\mathrm{tr}}$ is the mean route cost of public transport mode, and $\omega_{rs}^{\mathrm{pr}}$ is the mean route cost of P&R mode. The value of β should be calibrated based on real data and/or survey data in practice. In the numerical study, the value β follows that used in Shi et al. (2014).

The Logit-model is used to calculate the modal-split (three modes: private car, public transport, and P&R) as follows:

$$\frac{q_{rs}^{\mathrm{au}}}{Q_{rs}} = \frac{\exp\{-\beta\omega_{rs}^{\mathrm{au}}\}}{\exp\{-\beta\omega_{rs}^{\mathrm{au}}\}+\exp\{-\beta\omega_{rs}^{\mathrm{pr}}\}+\exp\{-\beta\omega_{rs}^{\mathrm{tr}}\}} \qquad (3)$$

$$\frac{q_{rs}^{\mathrm{tr}}}{Q_{rs}} = \frac{\exp\{-\beta\omega_{rs}^{\mathrm{tr}}\}}{\exp\{-\beta\omega_{rs}^{\mathrm{au}}\}+\exp\{-\beta\omega_{rs}^{\mathrm{pr}}\}+\exp\{-\beta\omega_{rs}^{\mathrm{tr}}\}} \qquad (4)$$

$$\frac{q_{rs}^{\mathrm{pr}}}{Q_{rs}} = \frac{\exp\{-\beta\omega_{rs}^{\mathrm{pr}}\}}{\exp\{-\beta\omega_{rs}^{\mathrm{au}}\}+\exp\{-\beta\omega_{rs}^{\mathrm{pr}}\}+\exp\{-\beta\omega_{rs}^{\mathrm{tr}}\}} \qquad (5)$$

where q_{rs}^{au}, q_{rs}^{tr}, q_{rs}^{pr} are the private car, public transport and P&R demands for OD pair (r, s), respectively. We use the logit-model here for simplicity. Other discrete choice models such as the C-logit model or probity model to better accommodate correlations among different modes can be readily incorporated into the overall modeling framework in this paper.

We now formulate the travel costs of the three modes. The public transport service is given and has a fixed running time for each OD pair. For OD pair $(r, s) \in RS$, the mean route cost of public transport users can be given as

$$\omega_{rs}^{\mathrm{tr}} = \alpha_1^{\mathrm{tr}} u_{rs}^{\mathrm{tr}}, \qquad (r,s) \in RS \qquad (6)$$

where u_{rs}^{tr} is the mean travel time, and α_1^{tr} converts the travel time into a cost for the public transport users. The value of α_1^{tr} should be calibrated with a combination of real data and survey data (survey is often used to quantify the stated preference of users) in practice. The value of α_1^{tr} used in the numerical studies in this paper follows Shi et al. (2014). We denote the route of the public transport as p_{rs}^{tr} for OD pair $(r, s) \in RS$.

An ATR scheme is represented as (D, γ, T), where denote $D \subset A^{\mathrm{au}}$ as the ATR area (including all road links that are closed to a proportion of travelers, i.e., restricting these travelers from

driving on the links), γ $(0 < \gamma < 1)$ is the restriction proportion of ATR scheme, i.e., the proportion of travelers who are not allowed to enter the ATR area D, and T is denoted as the set of P&R facilities locations. The restricted private car and P&R users R^{au} and R^{pr} can only travel in the subnetwork denoted by $(V, A^{\mathrm{au}} - D, A^{\mathrm{tr}})$.

For the non-restricted private car users N^{au}, let P_{rs}^{au} be the private car route set between OD pair (r, s) in network (V, A^{au}) and $P_{rs}^{\mathrm{au}} \neq \phi$. The route cost of non-restricted private car users N^{au} is:

$$c_{rsp}^{\mathrm{au}} = \sum_{a \in A^{\mathrm{au}}} t_a(x_a)\delta_{rs}^{ap} \qquad p \in P_{rs}^{\mathrm{au}}, (r,s) \in RS \tag{7}$$

where δ_{rs}^{ap} indicates the correspondence between the route and the link. If route p contains link a, $\delta_{rs}^{ap} = 1$; otherwise, $\delta_{rs}^{ap} = 0$.

The link travel time function of private car mode is as follows:

$$t_a(x_a) = t_{a0}\left[1 + \alpha\left(\frac{x_a}{c_a}\right)^m\right] \tag{8}$$

where for link a, t_{a0} is the free-flow travel time, c_a is the link capacity, α and m are two parameters in the link travel time function (e.g., $\alpha = 0.15, m = 4$).

For the non-restricted P&R users N^{pr}, let P_{rst}^{pr} be the route set for those with a transfer site at P&R facility t (also referred to as the "P&R transfer site" later on) between OD pair (r, s) in network G, then $P_{rst}^{\mathrm{pr}} = \{p + p_{ts}^{\mathrm{tr}} | p \in P_{rt}^{\mathrm{au}}\}$, where "$p + p_{ts}^{\mathrm{tr}}$" denotes a P&R travel route composed of private car route p and public transport route p_{ts}^{tr}. We further let $P_{rs}^{\mathrm{pr}} = \bigcup_{t \in T} P_{rst}^{\mathrm{pr}}$, which is the set of all P&R routes for OD pair (r, s). The cost of route p can be calculated as follows:

$$c_{rsp}^{\mathrm{pr}} = \sum_{a \in A^{\mathrm{au}}} t_a(x_a)\delta_{rs}^{ap} + u_{ts}^{\mathrm{tr}}, \qquad p \in P_{rst}^{\mathrm{pr}}, t \in T, (r,s) \in RS \tag{9}$$

For the restricted P&R users R^{pr}, similarly, let $\tilde{P}_{rst}^{\mathrm{pr}} = \{p + p_{ts}^{\mathrm{tr}} | p \in \tilde{P}_{rt}^{\mathrm{au}}\}$, i.e., the set of routes with a transfer site at P&R facility t, where $\tilde{P}_{rt}^{\mathrm{au}}$ is the set of routes between OD pair (r, t) in network $(V, A^{\mathrm{au}} - D)$. We further define $\tilde{P}_{rs}^{\mathrm{pr}} = \bigcup_{t \in T} \tilde{P}_{rst}^{\mathrm{pr}}$, i.e., the set of routes between O-D pair (r, s).

Let $RS^{\mathrm{pr}} = \{(r,s) \in RS: \tilde{P}_{rs}^{\mathrm{pr}} \neq \phi\}$ be the set of OD pairs which have at least one P&R route that is not blocked due to the ATR scheme, and let $RS \backslash RS^{\mathrm{pr}}$ be the set of OD pairs whose P&R travel routes are all blocked (due to the ATR scheme). For restricted P&R users with at least one P&R route not blocked, they may still choose P&R mode, and for potential restricted P&R users with no feasible P&R route, they can always choose a public transport route between OD pair (r, s) (they indeed will be public transport users), and their travel cost will be $\alpha_1^{\mathrm{tr}} u_{rs}^{\mathrm{tr}}$, where α_1^{tr} is a cost parameter converts the travel time to a cost.

For the restricted private car users R^{au}, $\tilde{P}_{rs}^{\mathrm{au}}$ is the route set for OD pair (r, s) in network $(V, A^{\mathrm{au}} - D)$, where $\tilde{P}_{rs}^{\mathrm{au}} \subset P_{rs}^{\mathrm{au}}$. For restricted private car users, if at least one driving route is feasible (not affected by the ATR scheme), they can still drive. Let $RS^{\mathrm{au}} = \{(r,s) \in$

RS: $\tilde{P}_{rs}^{\mathrm{au}} \neq \phi\}$ denote the set of OD pairs who have at least one driving route that is not blocked due to the ATR scheme. The private car route set is $\tilde{P}_{rs}^{\mathrm{au}}$, $(r,s) \in RS^{\mathrm{au}}$, and the route cost $\tilde{c}_{rsp}^{\mathrm{au}}$ of route $p \in \tilde{P}_{rs}^{\mathrm{au}}$ can be calculated by Eq. (7). For those OD pairs with all driving routes blocked by the ATR scheme, $\tilde{P}_{rs}^{\mathrm{au}} = \phi$, and we let $RS \backslash RS^{\mathrm{au}}$ denote the set of these OD pairs. The restricted private car users have to transfer to public transport or P&R mode (according to minimal route cost principle), and indeed they become public transport or P&R users. This consideration is similar to that in Shi et al. (2014). The route set for demand R^{au} is defined as $\tilde{P}_{rs}^{\mathrm{au}} = \tilde{P}_{rs}^{\mathrm{pr}} \cup \{p_{rs}^{\mathrm{tr}}\}$. The cost $\tilde{c}_{rsp}^{\mathrm{au}}$ of route p can be determined as follows:

$$\tilde{c}_{rsp}^{\mathrm{au}} = \sum_{a \in A^{\mathrm{au}} - D} t_a(x_a)\delta_{rs}^{ap} + \alpha_1^{\mathrm{tr}} u_{ts}^{\mathrm{tr}}, \qquad p \in \tilde{P}_{rst}^{\mathrm{pr}},\ t \in T \cup \{r\}, (r,s) \in RS \tag{10}$$

Following Shi et al. (2014), the user equilibrium conditions can be represented as a nonlinear complementary problem (NCP) in the following:

$$f_{rsp}^{\mathrm{au}}\left(c_{rsp}^{\mathrm{au}} - u_{rs}^{\mathrm{au}}\right) = 0, \qquad p \in P_{rs}^{\mathrm{au}}, (r,s) \in RS \tag{11}$$

$$\left(c_{rsp}^{\mathrm{au}} - u_{rs}^{\mathrm{au}}\right) \geq 0, \qquad p \in P_{rs}^{\mathrm{au}}, (r,s) \in RS \tag{12}$$

$$f_{rsp}^{\mathrm{au}} \geq 0, \qquad p \in P_{rs}^{\mathrm{au}}, (r,s) \in RS \tag{13}$$

$$\tilde{f}_{rsp}^{\mathrm{au}}\left(\tilde{c}_{rsp}^{\mathrm{au}} - \tilde{u}_{rs}^{\mathrm{au}}\right) = 0, \qquad p \in \tilde{P}_{rs}^{\mathrm{au}}, (r,s) \in RS^{\mathrm{au}} \tag{14}$$

$$\left(\tilde{c}_{rsp}^{\mathrm{au}} - \tilde{u}_{rs}^{\mathrm{au}}\right) \geq 0, \qquad p \in \tilde{P}_{rs}^{\mathrm{au}}, (r,s) \in RS^{\mathrm{au}} \tag{15}$$

$$\tilde{f}_{rsp}^{\mathrm{au}} \geq 0, \qquad p \in \tilde{P}_{rs}^{\mathrm{au}}, (r,s) \in RS^{\mathrm{au}} \tag{16}$$

$$\tilde{f}_{rsp}^{\mathrm{au}}\left(\tilde{c}_{rs\bar{p}}^{\mathrm{au}} - \tilde{u}_{rs}^{\mathrm{pt}}\right) = 0, \qquad p \in \bigcup_{t \in T \cup \{r\}} \tilde{P}_{rsp}^{\mathrm{pr}}, (r,s) \in RS \backslash RS^{\mathrm{au}} \tag{17}$$

$$\left(\tilde{c}_{rsp}^{\mathrm{au}} - \tilde{u}_{rs}^{\mathrm{pt}}\right) \geq 0 \qquad p \in \bigcup_{t \in T \cup \{r\}} \tilde{P}_{rsp}^{\mathrm{pr}}, (r,s) \in RS \backslash RS^{\mathrm{au}} \tag{18}$$

$$\tilde{f}_{rsp}^{\mathrm{au}} \geq 0, \qquad p \in \tilde{P}_{rst}^{\mathrm{pr}}, t \in T \cup \{r\}, (r,s) \in RS \backslash RS^{\mathrm{au}} \tag{19}$$

$$f_{rsp}^{\mathrm{pr}}\left(c_{rsp}^{\mathrm{pr}} - u_{rs}^{\mathrm{pr}}\right) = 0, \qquad p \in P_{rst}^{\mathrm{pr}}, t \in T, (r,s) \in RS \tag{20}$$

$$\left(c_{rsp}^{\mathrm{pr}} - u_{rs}^{\mathrm{pr}}\right) \geq 0, \qquad p \in P_{rst}^{\mathrm{pr}}, t \in T, (r,s) \in RS \tag{21}$$

$$f_{rsp}^{\mathrm{pr}} \geq 0, \qquad p \in P_{rst}^{\mathrm{pr}}, t \in T, (r,s) \in RS \tag{22}$$

$$\tilde{f}_{rsp}^{\mathrm{pr}}\left(\tilde{c}_{rsp}^{\mathrm{pr}} - \tilde{u}_{rs}^{\mathrm{pr}}\right) = 0, \qquad p \in \tilde{P}_{rst}^{\mathrm{pr}}, t \in T, (r,s) \in RS^{\mathrm{pr}} \tag{23}$$

$$\left(\tilde{c}_{rsp}^{\mathrm{pr}} - \tilde{u}_{rs}^{\mathrm{pr}}\right) \geq 0 \qquad p \in \tilde{P}_{rst}^{\mathrm{pr}}, t \in T, (r,s) \in RS^{\mathrm{pr}} \tag{24}$$

$$\tilde{f}_{rsp}^{\mathrm{pr}} \geq 0, \qquad p \in \tilde{P}_{rst}^{\mathrm{pr}}, t \in T, (r,s) \in RS^{\mathrm{pr}} \tag{25}$$

$$c_{rsp}^{\mathrm{au}} = \sum_{a \in A^{\mathrm{au}}} t_a(x_a)\delta_{rs}^{ap} \qquad p \in P_{rs}^{\mathrm{au}}, (r,s) \in RS \tag{26}$$

$$\tilde{c}_{rsp}^{\mathrm{au}} = \sum_{a \in A^{\mathrm{au}} - D} t_a(x_a)\delta_{rs}^{ap} \qquad p \in \tilde{P}_{rs}^{\mathrm{au}}, (r,s) \in RS^{\mathrm{au}} \tag{27}$$

$$\tilde{c}_{rsp}^{\mathrm{au}} = \sum_{a \in A^{\mathrm{au}} - D} t_a(x_a)\delta_{rs}^{ap} + u_{ts}^{\mathrm{tr}}, \qquad p \in \tilde{P}_{rst}^{\mathrm{pr}}, t \in T \cup \{r\}, (r,s) \in RS \backslash RS^{\mathrm{au}} \tag{28}$$

$$c_{rsp}^{\mathrm{pr}} = \sum_{a \in A^{\mathrm{au}}} t_a(x_a)\delta_{rs}^{ap} + u_{ts}^{\mathrm{tr}}, \qquad p \in P_{rst}^{\mathrm{pr}}, t \in T, (r,s) \in RS \backslash RS^{\mathrm{au}} \tag{29}$$

$$\tilde{c}_{rsp}^{\mathrm{pr}} = \alpha_1^{\mathrm{tr}} u_{rs}^{\mathrm{tr}} \qquad p \in P_{rst}^{\mathrm{pr}}, t \in T, (r,s) \in RS^{\mathrm{pr}} \tag{30}$$

$$\frac{q_{rs}^{au}}{Q_{rs}} = \frac{exp\{-\beta\omega_{rs}^{au}\}}{exp\{-\beta\omega_{rs}^{au}\}+exp\{-\beta\omega_{rs}^{pr}\}+exp\{-\beta\omega_{rs}^{tr}\}}, \qquad (r,s) \in \mathrm{RS} \tag{31}$$

$$\frac{q_{rs}^{tr}}{Q_{rs}} = \frac{exp\{-\beta\omega_{rs}^{tr}\}}{exp\{-\beta\omega_{rs}^{au}\}+exp\{-\beta\omega_{rs}^{pr}\}+exp\{-\beta\omega_{rs}^{tr}\}}, \qquad (r,s) \in \mathrm{RS} \tag{32}$$

$$\frac{q_{rs}^{pr}}{Q_{rs}} = \frac{exp\{-\beta\omega_{rs}^{pr}\}}{exp\{-\beta\omega_{rs}^{au}\}+exp\{-\beta\omega_{rs}^{pr}\}+exp\{-\beta\omega_{rs}^{tr}\}}, \qquad (r,s) \in \mathrm{RS} \tag{33}$$

$$\sum_{p \in P_{rs}^{\mathrm{au}}} f_{rsp}^{\mathrm{au}} = (1-\gamma) q_{rs}^{\mathrm{au}}, \qquad (r,s) \in RS \tag{34}$$

$$\sum_{p \in \tilde{P}_{rs}^{\mathrm{au}}} \tilde{f}_{rsp}^{\mathrm{au}} = \gamma q_{rs}^{\mathrm{au}}, \qquad (r,s) \in RS^{\mathrm{au}} \tag{35}$$

$$\sum_{t\in T\cup\{r\}}\sum_{p\in\tilde{P}_{rst}^{\mathrm{pr}}}\tilde{f}_{rsp}^{\mathrm{au}}=\gamma q_{rs}^{\mathrm{au}},\qquad (r,s)\in RS\backslash RS^{\mathrm{au}} \tag{36}$$

$$\sum_{t\in T}\sum_{p\in P_{rst}^{\mathrm{pr}}}f_{rsp}^{\mathrm{pr}}=(1-\gamma)q_{rs}^{\mathrm{pr}},\qquad (r,s)\in RS \tag{37}$$

$$\sum_{t\in T}\sum_{p\in\tilde{P}_{rst}^{\mathrm{pr}}}\tilde{f}_{rsp}^{\mathrm{pr}}=\gamma q_{rs}^{\mathrm{pr}},\qquad (r,s)\in RS^{\mathrm{pr}} \tag{38}$$

$$\omega_{rs}^{au}=\begin{cases}(1-\gamma)u_{rs}^{au}+\gamma\tilde{u}_{rs}^{au}, & (r,s)\in RS^{au}\\ (1-\gamma)u_{rs}^{au}+\gamma\tilde{u}_{rs}^{pt}, & (r,s)\in RS\backslash RS^{au}\end{cases} \tag{39}$$

$$\omega_{rs}^{tr}=\alpha_1^{tr}u_{rs}^{tr},\qquad (r,s)\in RS \tag{40}$$

$$\omega_{rs}^{pr}=\begin{cases}(1-\gamma)u_{rs}^{pr}+\gamma\tilde{u}_{rs}^{pr}, & (r,s)\in RS^{pr}\\ (1-\gamma)u_{rs}^{pr}+\gamma\alpha_1^{tr}u_{rs}^{tr}, & (r,s)\in RS\backslash RS^{pr}\end{cases} \tag{41}$$

The NCP in Eqs. (11)-(41) ensures that users will choose the routes with the minimum travel cost.

The user equilibrium conditions related to non-restricted private car users N^{au} include constraints (11)-(13) and (34). Constraint (34) represents the flow conservation, where $(1-\gamma)q_{rs}^{\mathrm{au}}$ is the number of non-restricted users and equals the sum of route flows f_{rsp}^{au} for each OD pair.

The conditions related to restricted private car users R^{au} include constraints (14)-(16) and (35) and (36). Constraint (35) is for the restricted users who still have at least one feasible driving route (not affected by the ATR scheme), which equals the sum of route flows $\tilde{f}_{rsp}^{\mathrm{au}}$ for private cars between OD pair $(r,s)\in RS^{au}$. Constraint (36) is for the restricted users with no feasible driving route (all blocked due to the ATR scheme). These travelers will use public transport, which equals the sum of route flows $\tilde{f}_{rsp}^{\mathrm{au}}$ for OD pair $(r,s)\in RS/RS^{au}$, where $t\in T\cup\{r\}$ is the transfer site.

The conditions related to non-restricted P&R users N^{pr} include constraints (17)-(19) and (37). Constraint (37) means that the non-restricted P&R users are $(1-\gamma)q_{rs}^{\mathrm{pr}}$, which equals the sum of route flows f_{rsp}^{pr} for each OD pair $(r,s)\in RS$.

The conditions related to restricted P&R users R^{pr} include constraints (23)-(25) and (38). Constraint (38) means that the restricted P&R users, which equals the sum of route flows $\tilde{f}_{rsp}^{\mathrm{pr}}$ for P&R users between OD pair $(r,s)\in RS^{\mathrm{pr}}$. It means that the restricted P&R users transfer to public transport with a new travel route $p\in\tilde{P}_{rst}^{\mathrm{pr}}$ between OD pair $(r,s)\in RS^{\mathrm{pr}}$, where $t\in T$ is the transfer site of P&R facility.

Constraints (11) - (13) are complementary conditions, which can be stated as follows:

$$\text{If } f_{rsp}^{\mathrm{au}}>0, \text{ then } c_{rsp}^{\mathrm{au}}-u_{rs}^{\mathrm{au}}=0, p\in P_{rs}^{\mathrm{au}}, (r,s)\in RS \tag{42}$$

$$\text{If } f_{rsp}^{au}=0, \text{ then } c_{rsp}^{au}-u_{rs}^{au}\geq 0, p\in P_{rs}^{au}, (r,s)\in RS \tag{43}$$

For a given route $p, p\in P_{rs}^{\mathrm{au}}$, if $f_{rsp}^{\mathrm{au}}=0$, constraint (11) holds, indicating that the route cost c_{rsp}^{au} must be greater than or equal to the OD specific minimum cost u_{rs}^{au} for private cars. If $f_{rsp}^{\mathrm{au}}>0$, $c_{rsp}^{\mathrm{au}}=u_{rs}^{\mathrm{au}}$, i.e., the route cost c_{rsp}^{au} is equal to minimum route cost u_{rs}^{au}. Similarly,

the conditions in Eqs. (14)-(25) ensures that travelers always choose the minimum cost route.

Following similar traffic assignment models (Cantarella, 1997) in the literature, the following optimization problem can be constructed that yields the equilibrium flow patterns defined before:

$$\begin{aligned}\min Z =& \sum_{a\in A^{\mathrm{au}}}\int_0^{x_a} t_a(x)\,dx + \alpha_1^{\mathrm{tr}}\sum_{(r,s)\in RS} u_{rs}^{\mathrm{tr}} q_{rs}^{\mathrm{tr}} \\ &+\alpha_1^{\mathrm{tr}}\sum_{(r,s)\in RS\setminus RS^{\mathrm{au}}}\sum_{t\in T\cup\{r\}} u_{ts}^{\mathrm{tr}}\sum_{p\in \tilde{P}_{rst}^{\mathrm{pr}}} \tilde{f}_{rsp}^{\mathrm{au}} \\ &+\alpha_1^{\mathrm{tr}}\sum_{(r,s)\in RS}\sum_{t\in T} u_{ts}^{\mathrm{tr}}\sum_{p\in P_{rst}^{\mathrm{pr}}} f_{rsp}^{\mathrm{pr}} \\ &+\alpha_1^{\mathrm{tr}}\sum_{(r,s)\in RS^{\mathrm{pr}}}\sum_{t\in T} u_{ts}^{\mathrm{tr}}\sum_{p\in \tilde{P}_{rst}^{\mathrm{pr}}} \tilde{f}_{rsp}^{\mathrm{pr}} \\ &+\alpha_1^{\mathrm{tr}}\sum_{(r,s)\in RS\setminus RS^{\mathrm{pr}}} \gamma u_{rs}^{\mathrm{tr}} q_{rs}^{\mathrm{pr}} \\ &+\frac{1}{\beta}\sum_{(r,s)\in RS}\left[q_{rs}^{\mathrm{au}}\ln\frac{q_{rs}^{\mathrm{au}}}{Q_{rs}} + q_{rs}^{\mathrm{tr}}\ln\frac{q_{rs}^{\mathrm{tr}}}{Q_{rs}} + q_{rs}^{\mathrm{pr}}\ln\frac{q_{rs}^{\mathrm{pr}}}{Q_{rs}}\right] \\ &+\frac{1}{\eta}\sum_{(r,s)\in RS} Q_{rs}\left(\ln\frac{Q_{rs}}{\bar{Q}_{rs}} - 1\right) \end{aligned} \tag{44}$$

s.t.

$$q_{rs}^{\mathrm{au}} + q_{rs}^{\mathrm{tr}} + q_{rs}^{\mathrm{pr}} = Q_{rs}, \qquad (r,s)\in RS \tag{45}$$

$$\sum_{p\in P_{rs}^{\mathrm{au}}} f_{rsp}^{\mathrm{au}} = (1-\gamma) q_{rs}^{\mathrm{au}}, \qquad (r,s)\in RS \tag{46}$$

$$\sum_{p\in \tilde{P}_{rs}^{\mathrm{au}}} \tilde{f}_{rsp}^{\mathrm{au}} = \gamma q_{rs}^{\mathrm{au}}, \qquad (r,s)\in RS^{\mathrm{au}} \tag{47}$$

$$\sum_{t\in T\cup\{r\}}\sum_{p\in \tilde{P}_{rst}^{\mathrm{pr}}} \tilde{f}_{rsp}^{\mathrm{au}} = \gamma q_{rs}^{\mathrm{au}}, \quad (r,s)\in RS\setminus RS^{\mathrm{au}} \tag{48}$$

$$\sum_{t\in T}\sum_{p\in P_{rst}^{\mathrm{pr}}} f_{rsp}^{\mathrm{pr}} = (1-\gamma) q_{rs}^{\mathrm{pr}}, (r,s)\in RS \tag{49}$$

$$\sum_{t\in T}\sum_{p\in \tilde{P}_{rst}^{\mathrm{pr}}} \tilde{f}_{rsp}^{\mathrm{pr}} = \gamma q_{rs}^{\mathrm{pr}}, \qquad (r,s)\in RS^{\mathrm{pr}} \tag{50}$$

$$f_{rsp}^{\mathrm{au}} \geq 0, \qquad p\in P_{rs}^{\mathrm{au}}, (r,s)\in RS \tag{51}$$

$$\tilde{f}_{rsp}^{\mathrm{au}} \geq 0, \qquad p\in \tilde{P}_{rs}^{\mathrm{au}}, (r,s)\in RS^{\mathrm{au}} \tag{52}$$

$$\tilde{f}_{rsp}^{\mathrm{au}} \geq 0, \qquad p\in \tilde{P}_{rst}^{\mathrm{pr}}, t\in T\cup\{r\}, (r,s)\in RS\setminus RS^{\mathrm{au}} \tag{53}$$

$$f_{rsp}^{\mathrm{pr}} \geq 0, \qquad p\in P_{rst}^{\mathrm{pr}}, t\in T, (r,s)\in RS \tag{54}$$

$$\tilde{f}_{rsp}^{\mathrm{pr}} \geq 0, \qquad p\in \tilde{P}_{rst}^{\mathrm{pr}}, t\in T, (r,s)\in RS^{\mathrm{pr}} \tag{55}$$

$$\begin{aligned} x_a =& \sum_{(r,s)\in RS}\sum_{p\in P_{rs}^{\mathrm{au}}} f_{rsp}^{\mathrm{au}}\delta_{rs}^{ap} + \sum_{(r,s)\in RS^{\mathrm{au}}}\sum_{p\in \tilde{P}_{rs}^{\mathrm{au}}} \tilde{f}_{rsp}^{\mathrm{au}}\delta_{rs}^{ap} + \sum_{(r,s)\in RS\setminus RS^{\mathrm{au}}}\sum_{p\in \tilde{P}_{rs}^{\mathrm{pr}}} \tilde{f}_{rsp}^{\mathrm{au}}\delta_{rs}^{ap} \\ &+\sum_{(r,s)\in RS}\sum_{p\in P_{rs}^{\mathrm{pr}}} f_{rsp}^{\mathrm{pr}}\delta_{rs}^{ap} + \sum_{(r,s)\in RS^{\mathrm{pr}}}\sum_{p\in \tilde{P}_{rs}^{\mathrm{pr}}} \tilde{f}_{rsp}^{\mathrm{pr}}\delta_{rs}^{ap} \end{aligned} \tag{56}$$

One can write down the Karush-Kuhn-Tucker conditions for the above optimization problem and verify the equivalency between the optimization problem and the NCP defined in Eqs. (11)-(41). The solution existence to the above optimization problem is ensured since all the functions are continuous, and the feasible solution set is compact. Moreover, due to the convexity of the objective function in Eq. (44), solutions of x_a, q_{rs}^{au}, q_{rs}^{tr}, q_{rs}^{pr}, Q_{rs} are unique. A similar gradient project algorithm as that in Shi et al. (2014) can be used to solve the optimization model, and the details are omitted here.

3. The bi-level model for optimizing the P&R facility locations and ATR scheme

This section further presents the bi-level model for optimizing the P&R facility locations and

ATR scheme, where the upper-level model optimizes the P&R facility location and ATR scheme, subject to the lower-level multimodal network equilibrium in Section 2. There is large body of literature on the bi-level problem in transportation, where one may refer to, e.g., Yang and Bell (1998), Gao et al. (2005), Liu et al. (2017), Huang et al. (2018), Fu et al. (2020) and Tran et al. (2021) for recent developments and related reviews.

In this study, we optimize the P&R facility locations and ATR scheme in order to (i) minimize total travel cost of users $z_T(\boldsymbol{x})$, (ii) minimize total emission cost $z_E(\boldsymbol{x})$, and (iii) maximize consumer surplus $z_C(\boldsymbol{Q})$ (or equivalently minimize $-z_C(\boldsymbol{Q})$), where $\boldsymbol{x}$ and $\boldsymbol{Q}$ are the vectors of link flow $\boldsymbol{x_a}$ and realized travel demand $\boldsymbol{Q_{rs}}$, which can be obtained from the lower-level multimodal network equilibrium model in Section 2. The decision variables include the restriction area D, the restriction ratio γ, and the P&R facility set T (set of nodes).

Specifically, the upper-level tri-objective optimization problem can be expressed as:

$$\min_{D,\gamma,T} \begin{pmatrix} z_T(\boldsymbol{x}) \\ -z_C(\boldsymbol{Q}) \\ z_E(\boldsymbol{x}) \end{pmatrix}$$

subject to

$$0 < \gamma \leq 1, D \subset A^{au}, T \subset T_0, \sum_{t \in T} C_t \leq C_0$$

where T is the set of P&R transfer facility locations; T_0 is the set of candidate P&R transfer facility locations; C_t is construction cost of P&R facilities at location t; C_0 is the P&R facility construction budget. We further formulate three efficiency metrics, i.e., total travel cost, total emission cost, and consumer surplus below.

Total travel cost is used to quantify the network efficiency for all users, including travel costs of users choosing private cars, public transport and P&R, i.e.,

$$\begin{aligned} z_T(\boldsymbol{x}) = & \sum_{a \in A^{au}} x_a t_a(x_a) + \alpha_1^{\mathrm{tr}} \sum_{(r,s) \in RS} u_{rs}^{\mathrm{tr}} q_{rs}^{\mathrm{tr}} + \alpha_1^{\mathrm{tr}} \sum_{(r,s) \in RS \setminus RS^{\mathrm{au}}} \sum_{t \in T \cup \{r\}} u_{ts}^{\mathrm{tr}} \gamma q_{rs}^{\mathrm{au}} \\ & + \alpha_1^{\mathrm{tr}} \left(\sum_{(r,s) \in RS} \sum_{t \in T} u_{ts}^{\mathrm{tr}} (1-\gamma) q_{rs}^{\mathrm{pr}} + \sum_{(r,s) \in RS^{\mathrm{pr}}} \sum_{t \in T} u_{ts}^{\mathrm{tr}} \gamma q_{rs}^{\mathrm{pr}} \right) \\ & + \alpha_1^{\mathrm{tr}} \sum_{(r,s) \in RS \setminus RS^{\mathrm{pr}}} u_{rs}^{\mathrm{tr}} \gamma q_{rs}^{\mathrm{pr}} \end{aligned} \tag{57}$$

The consumer surplus is used to measure the benefit of serving the demand. Similar to existing studies (Mankiw, 2003; Shi et al. 2014) and in line with the elastic demand function in Eq. (1), the consumer surplus can be calculated as follows:

$$z_C(Q) = \frac{1}{\eta} \sum_{(r,s)\in RS} Q_{rs} \tag{58}$$

Details regarding how to derive the above consumer surplus from the exponential elastic demand function is omitted (one may refer to Mankiw (2003)).

We now further formulate the emission cost. Vehicular emission has a direct impact on air quality, which becomes a major concern of many local authorities. There are three main pollutants from the vehicular emissions that have critical negative impacts on human health and the environment, i.e., carbon monoxide (CO), violate organic compounds (VOC), and nitrogen oxides (NOx) (Huang et al., 2020), which are considered in this paper to estimate the emission cost. The total emission cost is calculated by multiplying the traffic flow on each link by the link length (i.e., trip length on the link) and an emission factor. The emission factor is pollutant-specific and varies with traffic speeds, where an average speed is assumed across the whole link. In particular, a macroscopic TRANSYT-7F average-speed emission estimation model (Penic and Upchurch, 1992) is used to estimate the total emission cost, i.e.,

$$z_E(\boldsymbol{x}) = \sum_{y} \sum_{a\in A^{au}} \phi^y l_a x_a \frac{A^y e^{B^y \bar{S}_a}}{C^y \bar{S}_a} \tag{59}$$

where y is the pollutant, i.e., CO, VOC and NOx, and for link a, l_a is the link length, $\bar{S}_a$ is the average traffic speed (ft/s) and $\bar{S}_a = 20$ ft/s in this paper, x_a is the link flow (veh/hour), A^y, B^y and C^y are constant parameters, and ϕ^y ($/g) converts the damage from pollutant y to monetary equivalent. The emission cost parameters of Eq. (59) are listed in Table 1 (Penic and Upchurch, 1992), where the units ensure consistency between the traffic model and the emission estimation model (Castillo et al., 2014). Moreover, the monetary value is based on U.S. currency at its value in 1991 for consistency.

Table 1. Parameters for emission cost estimation

Parameters	Type of pollutant		
	CO	VOC	NOX
A^n(g/ft per veh)	3.3963	2.7843	1.5718
B^n(s/ft)	0.014561	0.015062	0.040732
C^n(s/ft)	1,000	10,000	10,000
ϕ^n($/gram)	0.00051	0.00136	0.00103

4. Solution algorithm

In this section, we elaborate the algorithm to solve the tri-objective bi-level model for optimizing the P&R facility locations and ATR scheme. The proposed bi-level model is non-

convex, and the number of feasible solutions increases exponentially with respect to the network size. It is extremely difficult (if not impossible) for traditional exact methods to obtain the optimal solution. Therefore, this paper adopts metaheuristic to solve the bi-level model. In particular, as the bi-level model contains complex underlying models, the parallel feature of genetic algorithm can greatly improve the computation efficiency (Cipriani et al., 2010; Wong et al., 2001). In addition, the studied problem is a multi-objective problem. The non-dominated sorting genetic algorithm with elite strategy (NSGA-II) was used to solve multi-objective model. Deb et al. (2002) proposed NSGA-II, and compared it with two other multi-objective evolutionary algorithms, i.e., Pareto-archived evolution strategy (PAES) and strength-Pareto evolutionary algorithms (SPEA). Deb et al. (2002) indicated that NSGA-II has significant advantages in solving multi-objective problem in terms of a fast non-dominated sorting procedure, an elitist strategy, a parameter-less approach and a simple but efficient constraint-handling method. Given its advantages, NSGA-II is used in this paper to solve the bi-level model and obtain the pareto optimal solution set. We briefly summarize the major coding frameworks in relation to NSGA-II below.

(i) We have binary codes indicating whether the node v, $v \in V$ is restricted or not, with each gene position corresponding to a node. If the node v is in the restriction area, the value of the gene position is one, and otherwise zero. In practice, for ease of implementation, the traffic manager usually sets the restriction area D as a single connected district or a limited number of multiple-connected district. A similar method as Zhang and Yang (2004) for determining the cordon locations for tolling is used to search for feasible ATR area D in this study. In particular, the node-link incidence matrix will be used. The node-edge incidence matrix Ω_G of an n-node, l-edge graph G without self-loop links is a matrix of order $n \times l$ such that $\Omega_G = [v_{ij}]$, and

$$v_{ij} = \begin{cases} 1, & \text{if link } j \text{ is incident at node } i, \text{and direction from node } i \\ 0, & \text{if link } j \text{ is not incident at node } i \\ -1, & \text{if link } j \text{ is incident at node } i, \text{and direction to node } i \end{cases}$$

In the above matrix each row corresponds to a node and each column corresponds to an edge. If the rank of Ω_G equal to $n-2$, the graph G is divided into two parts, i.e., the restriction area D and non-restriction area, and the restriction area D is a single connected area.

(ii) Under the allowable error σ, the binary discrete codes are used to represent the restriction ratio γ in the continuous interval [0,1], where $\sigma = 1/2^6$ in this study.

(iii) The codes indicating whether the node $t \in T_0$ is selected as a P&R facility location, where each gene position corresponds to a node. If $t \in T$, the value of the gene position is one, and otherwise zero.

In summary, each chromosome with the relevant code described above uniquely determines

the particular design of P&R facility and ATR scheme. The link flows x_a can obtained from the lower-level network equilibrium model, based on which we can evaluate the three objectives of user travel cost, emission cost and consumer surplus.

The detailed process of NSGA-II is summarized below:

Input: Transport network G; travel demand $Q_{rs}, (r,s) \in RS$; the time cost of free flow $t_{a0}, a \in A$; the number of nodes n for network G; the maximal number of generations H; the population size M; the crossover probability S_c; the mutation probability S_m.

Output: Pareto frontier that contains multiple Pareto optimal solutions (tri-objective).

Step 0: Initialization

Set the generation counter $h = 0$;

Randomly generate the parent population Φ_h;

Set the offspring population $\Psi_h = \emptyset$;

Calculate the flow distribution in the network using the gradient project algorithm for each element in Φ_h.

Calculate the three objective values of each element in Φ_h using Eqs. (57)-(59).

Step 1: Main loop

Set $R_h = \Phi_h \cup \Psi_h$;

Use the algorithm of fast-non-dominated-sort to sort R_h into different non-domination levels $F = (F_1, F_2, \dots)$;

Perform the selection:

Set $\Phi_{h+1} = \emptyset$;

While $|\Phi_{h+1}| + |F_i| \leq M$, do

Set $\Phi_{h+1} = \Phi_{h+1} \cup F_i$;

Set $i = i + 1$.

Calculate the crowding distance for each element in F_i using the algorithm of crowding-distance-assignment;

Sort F_i in the descending order of the crowding distance;

Select the first $M - |\Phi_{h+1}|$ elements of F_i and denote as $F_i(M - |\Phi_{h+1}|)$;

Set $\Phi_{h+1} = \Phi_{h+1} \cup F_i(M - |\Phi_{h+1}|)$.

Perform the crossover and mutation to generate the offspring population Ψ_{h+1};

Calculate the flow distribution in the network using the gradient project algorithm for each element in Ψ_{h+1}.

Calculate the three objective values of each element in Ψ_{h+1} using Eqs. (57)-(59).

Step 2: Stopping criterion

Set $h = h + 1$;

If $h \leq H$, then return to Step 1; otherwise,

Set $R_h = \Phi_h \cup \Psi_h$;

Use the algorithm of fast-non-dominated-sort to sort R_h into different non-domination

levels $F = (F_1, F_2, \ldots)$;

Obtain the Pareto-frontier approximation F_1 and stop.

If the algorithm generated unfeasible solutions (e.g., the ATR area is not a single connected one, or the total construction cost is beyond C_0 in the step of initialization) during the crossover operation and mutation operation, a random feasible solution will be generated to replace it.

5. Numerical study

5.1 A small network example

This section uses one numerical example to illustrate applicability of the proposed model and solution approach. We consider a network in Figure 1 that consists of 27 nodes, 44 links and 18 district units (U1-U28 in Figure 1). The node-22 is the airport station. The demand levels of OD pairs in this network vary from zero to 1791, the average demand is 185.7627 per OD pair.

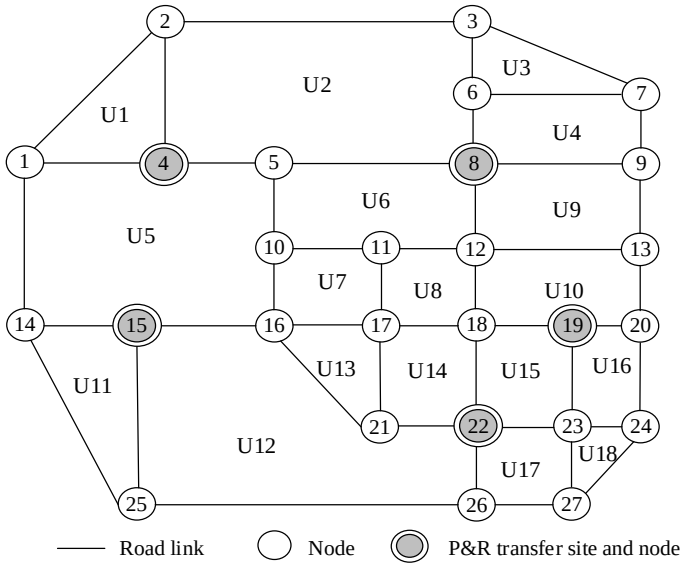

Figure 1. The layout of a small road network

The free-flow time t_{a0} and the link capacity c_a of all the links are summarized in the Table 2. The travel time of public transport u_{rs}^{tr} is assumed as 1.25 times the travel time of the shortest driving route for OD pair $(r, s) \in RS$. The available budget is 12 million for construction of P&R facilities. The airport must set up a P&R transfer station, i.e., the node-22 is a fixed location of P&R facility. The construction costs of P&R facilities for different locations in the network are summarized in Table 3.

Table 2. Free flow travel time and link capacity

link	t_{a0} (min)	c_a (pcu/h)	link	t_{a0} (min)	c_a (pcu/h)	link	t_{a0} (min)	c_a (pcu/h)
1-2	3.5	2,730	1-4	2.8	2,280	1-14	3.0	2,730
2-4	3.1	1,775	3-6	1.5	2,525	3-7	3.5	2,894
5-8	3.2	2,352	5-10	1.3	2,184	6-7	3.1	1,502
7-9	1.2	2,894	8-9	3.5	2,352	8-12	1.2	2,525
2-3	3.7	2,800	11-17	1.2	2,663	11-12	1.0	2,066
4-5	1.2	2,280	14-15	1.3	1,774	13-20	1.3	2,894
6-8	1.3	2,525	16-17	1.1	2,384	15-25	3.8	1,975
9-13	1.4	2,894	18-19	1.3	2,384	17-21	3.0	2,633
10-11	1.2	2,066	10-16	1.5	2,184	19-23	3.4	855
12-13	2.5	2,066	12-18	1.0	2,525	22-26	2.2	2,604
14-25	3.5	2,730	15-16	1.2	2,269	25-26	4.3	2,894
16-21	4.5	2,114	17-18	1.1	2,384	20-24	3.5	2,894
18-22	3.2	2,352	19-20	1.5	2,384	23-24	3.5	1,694
21-22	1.3	1,694	22-23	1.1	1,694	26-27	1.1	2,894
23-27	2.4	855	24-27	3.2	2,894			

Table 3. Construction cost of parking facilities at potential P&R locations

Node	Construction cost ($US)	Node	Construction cost ($US)	Node	Construction cost ($US)
1	1,568,600	10	2,026,200	19	1,978,000
2	1,813,700	11	2,427,800	20	1,561,800
3	1,437,500	12	2,474,900	21	1,464,400
4	2,871,200	13	1,213,100	22	1,515,700
5	2,421,000	14	1,210,500	23	1,696,500
6	1,719,900	15	1,719,900	24	1,061,800
7	1,974,900	16	2,072,300	25	1,186,100
8	1,815,700	17	2,174,900	26	1,261,800
9	1,437,500	18	2,217,300	27	1,382,800

The algorithms were coded through the platform MATLAB (R2020b) and tested on a PC with Intel® Core (TM) 3.0 GHz processor and 16.00 GB RAM and Windows 10 Home Edition operating system(64-bit).

For the NSGA-II algorithm, the population size $M = 60$, the crossover probability $S_c = 0.9$, and the mutation probability $S_m = 0.09$. In terms of stopping criterion, the maximum number of the generation updating is 500.

5.1.1 The benchmark case

The case without ATR scheme and with P&R facility at location/node $\{4, 8, 15, 19, 22\}$ is set as the benchmark case. We solve the multimodal network equilibrium and calculate the total travel demand and the modal-split, as well as the total travel cost, consumer surplus and total emission cost, which are summarized in Table 4. When the ratio of flow to capacity on a road link is greater than one, we regard it as a congested link. The number of congested link (NCL) in the benchmark case is 14, which is also summarized in Table 4 (as an efficiency metric).

To ease the presentation, we define the following abbreviations: TTD = total travel demand; TCF = total car flow; TPTF = total public transport flow; TPRF = total P&R flow; AS=car mode share; PTS = public transport mode share; PRS=P&R mode share; TLC=total link cost; CS= consumer surplus; TEC = total emission cost; NCL = number of congested links; T = the set of P&R facility locations (nodes).

Table 4. The travel demand, modal-split, and system efficiency metrics

TTD	TCF	TPTF	TPRF	AS	PTS	PRS
159266.83	96883.6	51470.02	10913.21	60.83%	32.32%	6.85%
TLC	CS	TEC	NCL		T	
416407.37	3185336.79	87029.14	14		4,8,15,19,22	

In the next subsections, we explore several different scenarios where the optimization problem might be subject to additional physical constraints or the construction costs for P&R facilities may vary. Section 5.1.2 optimizes P&R facility location under given ATR scheme; Section 5.1.3 optimizes the ATR scheme under given P&R facility locations; Section 5.1.4 jointly optimizes P&R facility location and ATR scheme; Section 5.1.5 optimizes the ATR restriction area and P&R facility location under constrained restriction ratio (e.g., $\gamma = 0.2$ and $\gamma = 0.5$). The scenario "Optimization of P&R facility location under a given ATR scheme" in Section 5.1.2 and the scenario "Optimization of the ATR scheme under given P&R facility location" in Section 5.1.3 will be compared against the scenario "Joint optimization of P&R facility locations and ATR scheme" in Section 5.1.4 to evaluate the additional benefit from integrating ATR scheme optimization (compared to optimizing P&R facilities only) and the additional benefit from integrating P&R facility location optimization (compared to optimizing ATR scheme only), respectively. Moreover, the scenario "Optimization of P&R facility locations and restriction area under given restriction ratios" in Section 5.1.5 will be compared to the scenario "Joint optimization of P&R facility location and ATR scheme" in Section 5.1.4 to evaluate the efficiency loss due to a constrained restriction ratio in the ATR scheme.

5.1.2 Optimization of P&R facility location under a given ATR scheme

This subsection optimizes the P&R facility location under given restriction ratio and restriction area for the ATR scheme. The solution Pareto frontier (tri-objective) is obtained, and then three solutions along the Pareto frontier with different preference over the three objectives are used for illustration. We will also compare the results of optimizing P&R facility location with the fixed ATR scheme with those of the benchmark scheme.

The ATR scheme is given as follows. The fixed restriction area includes the following links: 5-8, 5-10, 8-12, 10-11, 10-16, 11-12, 11-17, 12-18, 16-17, 17-18, 17-21, and the restriction

ratio is γ= 0.2. The Pareto frontier (in terms of tri-objective optimization) for optimizing P&R facility location given the ATR scheme are illustrated in Figure 2. The Pareto frontier is displayed in a three-dimensional scatter plot, and also illustrated through three two-dimensional scatter plots. One can observe the clear trade-off among minimizing total travel cost, maximizing consumer surplus, and minimizing total emission cost.

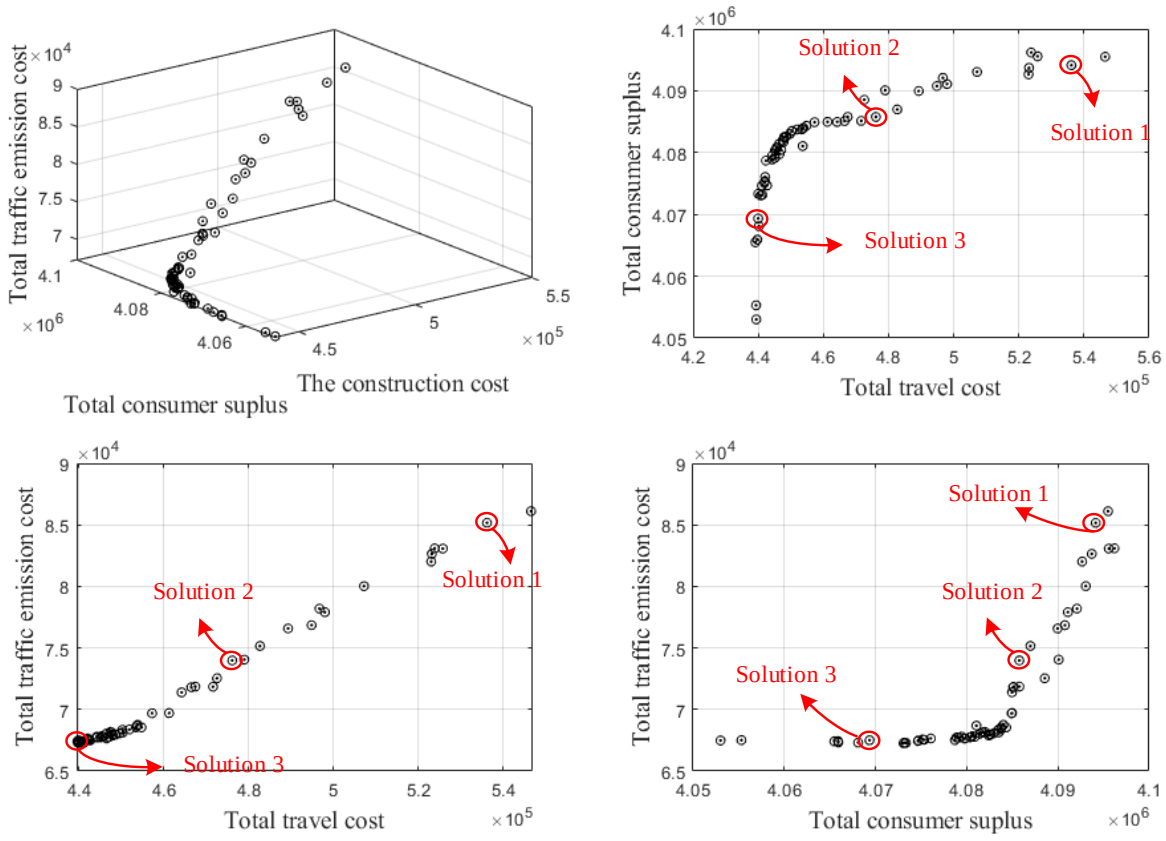

Figure 2. Pareto frontier: optimization of P&R facility location under given ATR scheme

The three objectives considered in this paper indeed may conflict with each other. Three different solutions on the Pareto frontier (marked by large circles in Figure 2) with different preferences over the three objectives are used to illustrate the differences in the solutions when the preferences over the three objectives vary. In particular, Solution 1 concerns mainly the consumer surplus, Solution 3 concerns mainly the emission cost and travel cost, and Solution 2 concerns more equally the three objectives. For the three solutions, Figure 3 shows the optimal P&R facility locations given the same ATR scheme. The solid orange areas in Figure 3 indicate the restriction area, where the restricted road links are indicated as dashed lines. In addition, the nodes in solid blue are optimal P&R facility locations. It is noteworthy that all driving routes are blocked between OD pair (17,19) due to the ATR scheme. These travelers have to transfer to public transport or P&R mode.

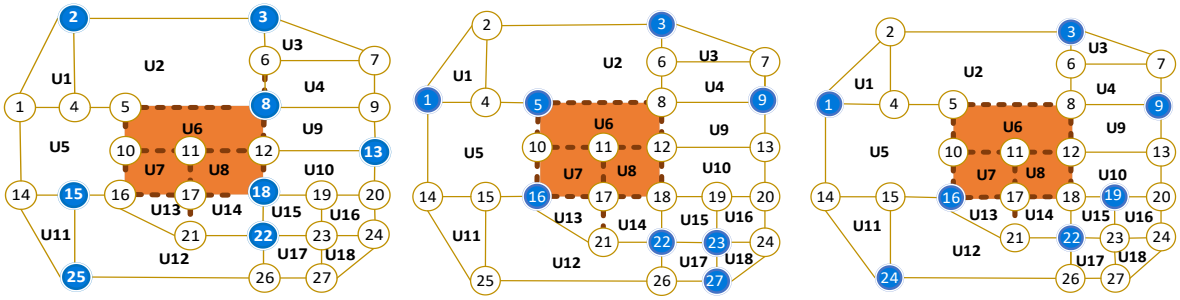

(a) solution 1 ($\gamma = 0.2$) (b) solution 2 ($\gamma = 0.2$) (c) solution 3 ($\gamma = 0.2$)

Figure 3. Optimal locations for P&R facilities under a given ATR scheme (solid orange area: restriction area; dashed lines: restricted road links; solid blue nodes: P&R facility locations)

The travel demand, modal-split, and system efficiency metrics for the three solutions in Figure 3 are summarized in Table 5. These results clearly demonstrate that optimizing of P&R facility location even if ATR scheme is given is useful, where congestion and emission costs can be reduced (e.g., when compared with benchmark case in Table 4).

Table 5. The travel demand, modal-split, and system efficiency metrics under the three solutions in Figure 2

solution	TTD	TCF	TPTF	TPRF	AS	PTS	PRS
1	163235.00	96033.47	55456.87	11744.66	59%	34%	7%
2	163446.60	91624.56	57386.05	14435.99	56%	35%	9%
3	163576.02	88945.59	58073.15	16557.28	54%	36%	10%
solution	TLC	CS	TEC	NCL	*T*		
1	523130.03	4093713.67	82640.97	6	2,3,8,13,15,18,22,25		
2	472553.57	4088550.41	72540.78	5	1,3,5,9,16,22,23,25		
3	440735.36	4073070.51	67266.14	3	1,3,9,16,19,22,24		

5.1.3 Optimization of ATR scheme under given P&R facility location

This subsection optimizes the restriction ratio and restriction area for the ATR scheme under given P&R facilities. Similar to Section 5.1.2, the solution Pareto frontier (tri-objective) is obtained, and then three solutions along the Pareto frontier with different preferences over the three objectives are used for illustration. We will also compare "optimizing ATR scheme under given P&R facilities" with the benchmark case in Section 5.1.1.

The P&R facilities are identical to those in the benchmark case. The fixed P&R facility locations include (nodes) $\{4, 8, 15, 19, 22\}$. The solution Pareto frontier (in terms of tri-objective optimization) for optimizing the ATR scheme given P&R facility location are illustrated in Figure 4. The Pareto frontier is displayed in a three-dimensional scatter plot, and also illustrated through three two-dimensional scatter plots. Again, we can observe clear trade-offs among minimizing total travel cost, maximizing consumer surplus, and minimizing total

emission cost.

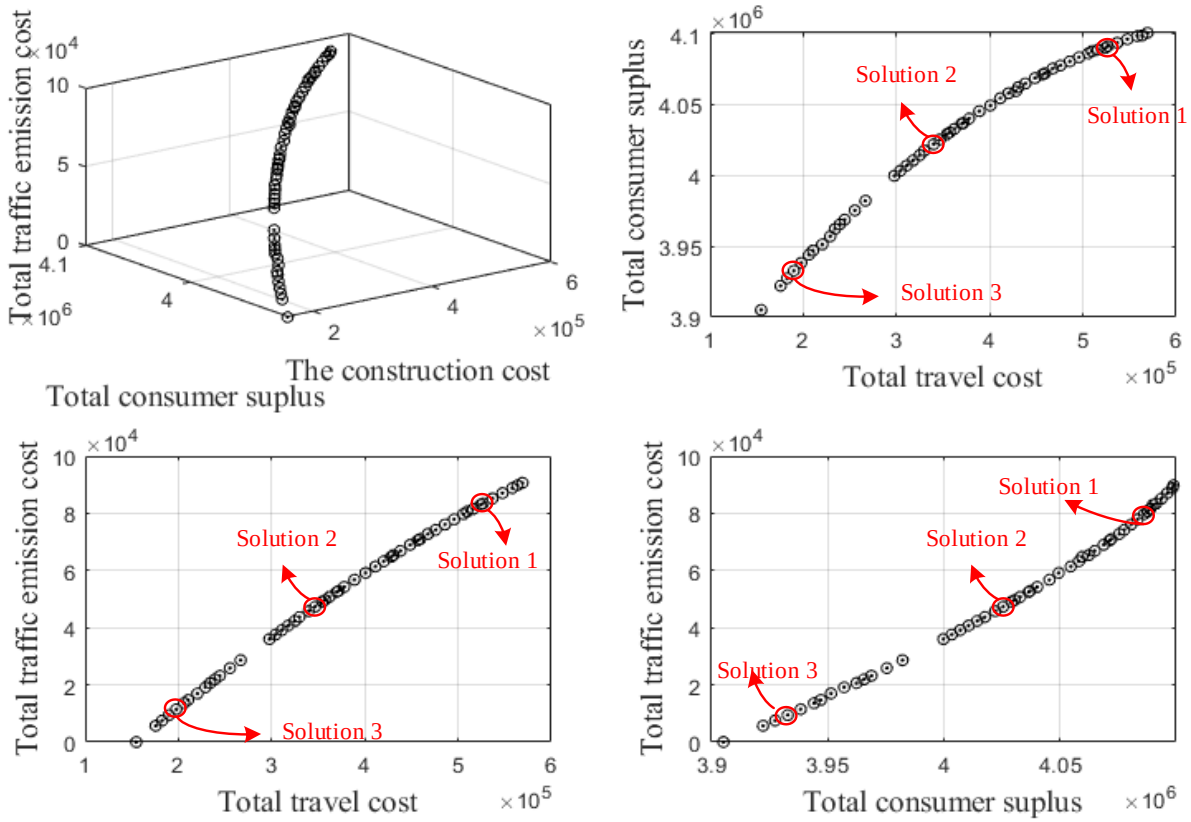

Figure 4. Pareto frontier: optimization of ATR scheme under given P&R facility location

Similarly, Solution 1 concerns mainly the consumer surplus, Solution 3 concerns mainly the emission cost and travel cost, and Solution 2 concerns more equally the three objectives. For the three solutions, Figure 5 shows the optimal ATR scheme under the same given P&R facilities (the details of the restriction area and restriction ratio are summarized in Table 6). The solid orange areas in Figure 5 indicate the restriction area, where the restricted road links are indicated as dashed lines. In addition, the nodes in solid blue are optimal P&R facility locations. The three solutions associate with different ATR restriction areas, indicating that the ATR scheme should be properly designed in order to achieve a specific objective.

Table 6. The restriction area and the restriction ratio under three solutions in Figure 4

Solution	ATR area	Restriction ratio
1	4-5,5-8,5-10,10-11,11-12,8-12,10-16,11-17,12-18,16-17,17-18,18-19,17-21,18-22,18-19,19-23,21-22,22-23	0.1429
2	4-5,5-8,5-10,10-11,11-12,8-12,10-16,11-17,12-18,15-16,16-17,17-18,16-21,17-21	0. 3651
3	6-8,8-9,8-12,9-3,11-12,12-13,12-18,17-18,18-19,19-20,13-20,18-22,19-23,22-23	0.7143

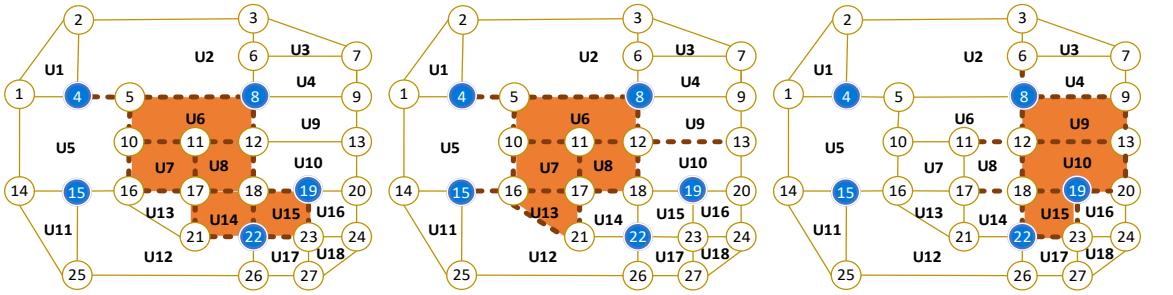

(a) solution 1 ($\gamma = 0.1429$) (b) solution 2 ($\gamma = 0.3651$) (c) solution 3 ($\gamma = 0.7143$)

Figure 5. Optimization ATR scheme under given P&R facilities locations (orange area: restriction area; dashed lines: restricted road links; solid blue nodes: P&R facility locations)

The travel demand, modal-split, and system efficiency metrics for the three solutions in Figure 5 are summarized in Table 7. These results demonstrate that optimizing ATR scheme even if P&R facilities are given can still be useful (while it is less efficient than the joint optimization in Section 5.1.4), where congestion and emission costs can be reduced (e.g., when compared with benchmark case in Table 4).

Table 7. The travel demand, modal-split, and system efficiency metrics under the three solutions in Figure 4

solution	TTD	TCF	TPTF	TPRF	AS	PTS	PRS
1	163746.65	98078.54	54013.71	11654.40	60%	33%	7%
2	161165.41	84910.71	63010.03	13244.68	53%	39%	8%
3	157533.37	63142.32	80684.04	13707.02	40%	51%	9%
solution	TLC	CS	TEC	NCL		*T*	
1	536732.04	4093666.25	85134.32	7		4,8,15,19,22	
2	394360.41	4047477.61	57796.16	5		4,8,15,19,22	
3	197815.06	3938334.29	11470.88	3		4,8,15,19,22	

5.1.4 Joint optimization of P&R facility location and ATR scheme

This subsection optimizes the P&R facility location and ATR scheme simultaneously. Similar to those in Section 5.1.2 and Section 5.1.3, we plot the solution Pareto frontier in Figure 6, and illustrate three solutions (on the solution Pareto frontier) with different preferences over the three objectives in Figure 7 and Table 8 (the three solutions are marked by red circles in Figure 6), and summarize the travel demand, modal-split, and system efficiency metrics for the three optimal solutions in Table 9.

By comparing Figure 6 for joint optimization of P&R facility locations and ATR scheme with Figure 2 for optimization of P&R facility locations under a given ATR scheme and Figure 4 for optimization of the ATR scheme under given the P&R facilities, one can identify that when the consumer surplus is identical, the total travel cost and total emission costs in Figure 6 are smaller, which means that joint optimization of P&R facility location and ATR scheme

dominates the "optimization of P&R facilities location under a given (non-optimal) ATR scheme" and the "optimization of ATR scheme under given (non-optimal) P&R facility locations". This also highlights the potential benefit from integrating ATR scheme optimization (compared to optimizing P&R facilities only) and the potential benefit from integrating P&R facility location optimization (compared to optimizing the ATR scheme only).

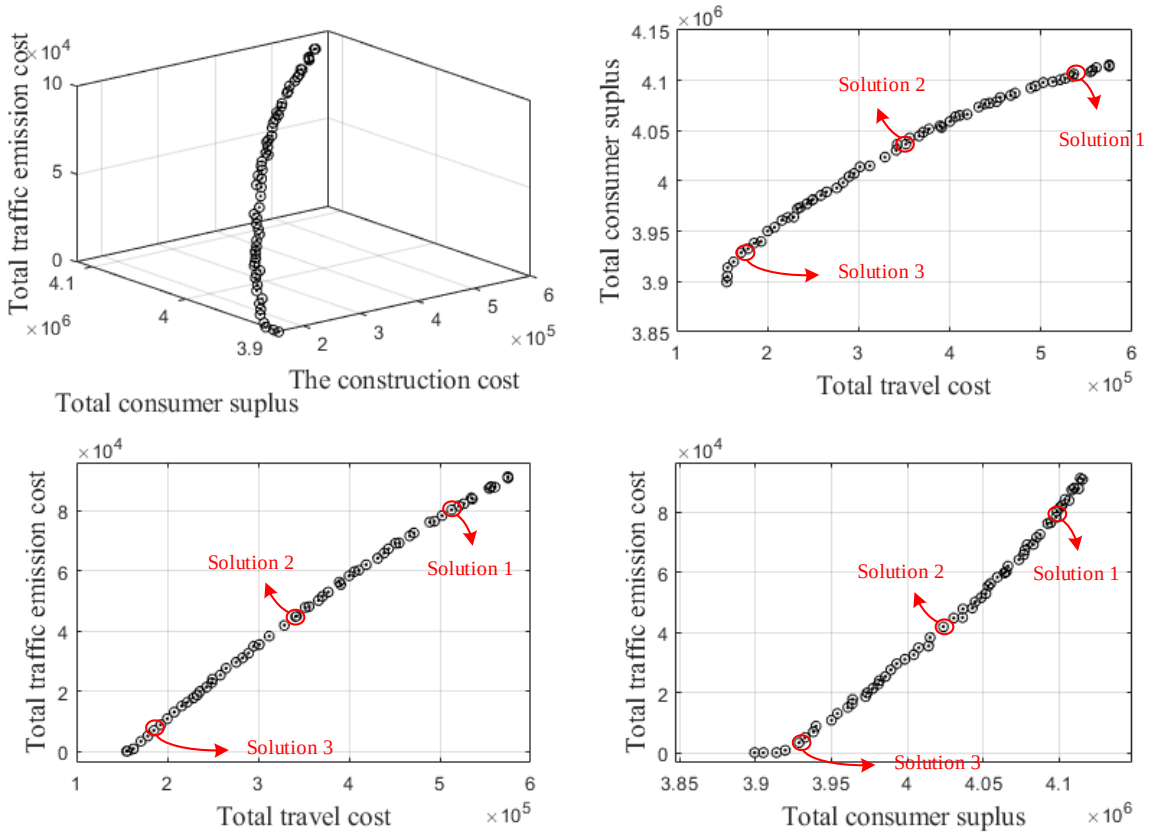

Figure 6. Pareto frontier: joint optimization of P&R facility location and ATR scheme

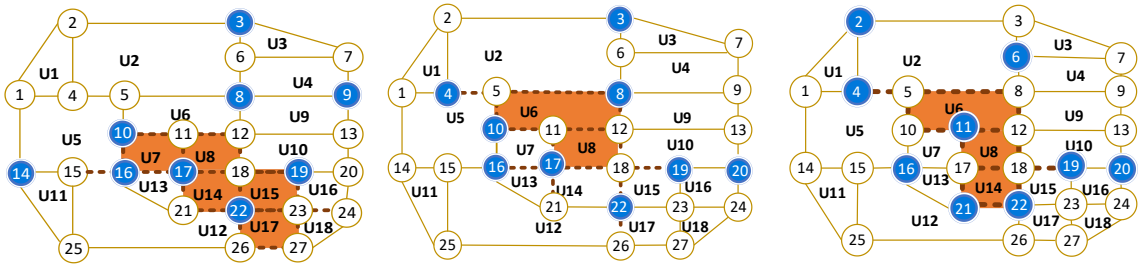

(a) solution 1 ($\gamma = 0.1635$) (b) solution 2 ($\gamma = 0.3810$) (c) solution 3 ($\gamma = 0.6571$)

Figure 7. Joint optimization of P&R facility location and ATR scheme (solid orange area: restriction area; dashed lines: restricted road links; solid blue nodes: P&R facility locations)

Table 8. The restriction area and the restriction ratio under three solutions in Figure 6

Solution	ATR area	Restriction ratio
1	10-11,10-16,11-12,11-17,12-18,15-16,16-17,17-18,18-19,17-21,18-22,19-23,21-22, 22-23,23-24, 23-26,26-27	0.1635
2	4-5,5-8,8-12,5-10,10-11, 11-12,11-17,12-18,16-17,17-18,17-21,18-22,18-19,22-26	0. 3810
3	4-5,5-8,5-10,8-12,10-11,11-12, 11-17,12-28,17-18,18-19,17-21,18-22,21-22	0.6571

Table 9. The travel demand, modal-split, and system efficiency metrics under the three solutions in Figure 6

Solution	TTD	TCF	TPTF	TPRF	AS	PTS	PRS
1	164281.63	93790.40	52228.59	18262.64	57.09%	31.79%	11.12%
2	161579.25	80921.89	61257.99	19399.37	50.08%	37.91%	12.01%
3	157684.24	57721.45	79930.17	20032.63	36.61%	50.69%	12.70%
Solution	TLC	CS	TEC	NCL	T		
1	534443.98	4102948.27	83716.80	5	3,8,9,10,14,16,17,19,22		
2	353273.18	4039481.20	47945.13	0	3,4 ,8,10,16,17,19,20,22		
3	190082.46	3942105.99	7941.38	0	2,4,6,11,16,19,20,21,22		

By comparing Table 9 for joint optimization of P&R facility location and ATR scheme with Table 5 for optimization of P&R facilities location under a given ATR scheme and Table 7 for optimization of ATR scheme under given P&R facility location, the observations of Figure 6 are consistent with those from comparison between Figure 4 and Figure 2. Given similar consumer surplus, the total travel cost and total emission cost are both smaller in Table 9 when compared to Table 5 and Table 7. This is partially due to that more travelers will shift to public transport or P&R (as can be observed from the two tables). The joint optimization of P&R facility location and ATR scheme further helps alleviate congestion and reduce vehicular emission.

5.1.5 Optimization of P&R facility location and restriction area under given restriction ratios

We now consider scenarios where the restriction ratio in the ATR scheme is subject to certain practical constraints, i.e., the restriction ratio is fixed. We then only optimize the P&R facility location and restriction area, but take the restriction ratio as given. We consider two cases: $\gamma = 0.5$ (e.g., even-odd vehicle license plate number-based restriction) and $\gamma = 0.2$ (restriction of two digits based on the last digit of the vehicle license plate numbers).

Similar to those in Section 5.1.2 and Section 5.1.3, we plot the solution Pareto frontier for both $\gamma = 0.5$ and $\gamma = 0.2$ in Figure 8, and illustrate three different solutions for $\gamma = 0.5$ and three different solutions for $\gamma = 0.2$ in Figure 9 (the three solutions for $\gamma = 0.5$ are marked by red circles and the three solutions for $\gamma = 0.2$ are marked by red circles in Figure 8), and

summarize the travel demand, modal-split, and system efficiency metrics for the six optimal solutions (three for $\gamma = 0.5$ and three for $\gamma = 0.2$) in Table 10.

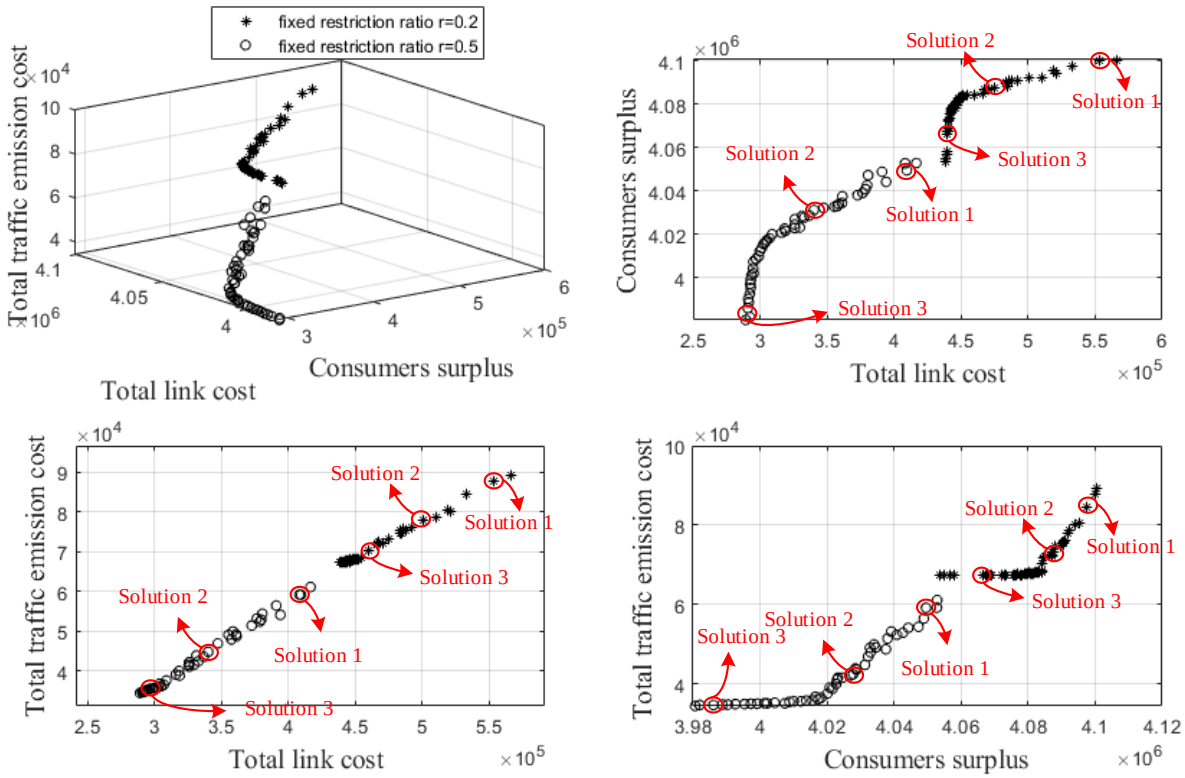

Figure 8. Optimization of P&R facility location and restriction area under given a restriction ratio of $\gamma = 0.2$ or $\gamma = 0.5$

By comparing the two cases with different restriction ratios ($\gamma = 0.2$ or $\gamma = 0.5$), it is obvious that the total travel cost and total emission cost are much smaller under a higher restriction ratio $\gamma = 0.5$, as shown in Figure 8. This is because that under a larger restriction ratio more traffic transfers to P&R and public transport. It follows that the restriction ratio $\gamma = 0.5$ yields less congestion when compared to $\gamma = 0.2$, while it also yields less travel (and thus less consumer surplus), as can be seen in Table 10. Overall, while the ATR scheme under restriction ratio constraints will lose some efficiency, the optimization of P&R location and ATR area can still help substantially reduce traffic congestion and emission.

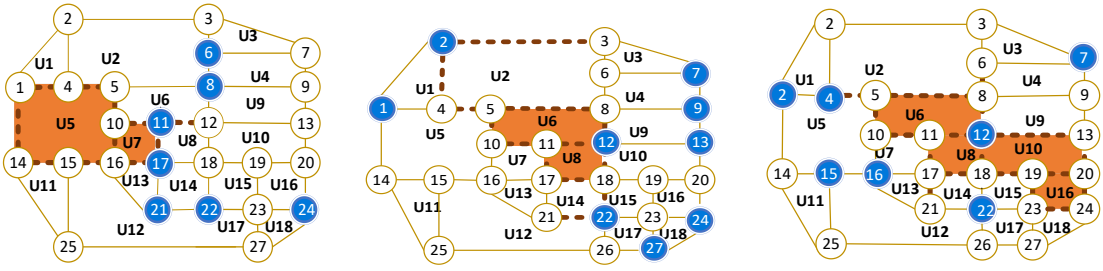

(a) solution 1 ($\gamma = 0.2$) (b) solution 2 ($\gamma = 0.2$) (c) solution 3 ($\gamma = 0.2$)

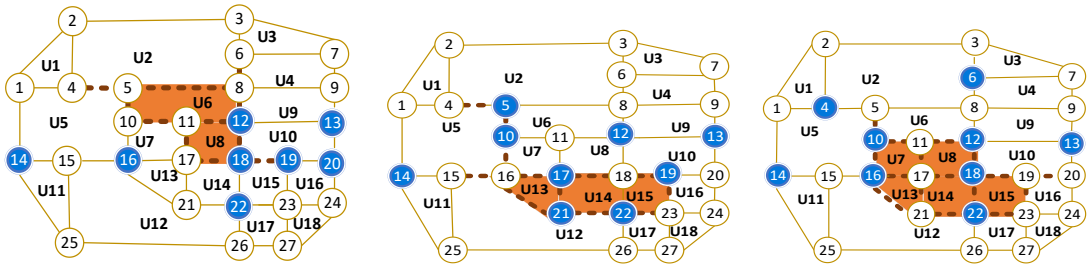

(d) solution 1 ($\gamma = 0.5$) (e) solution 2 ($\gamma = 0.5$) (f) solution 3 ($\gamma = 0.5$)

Figure 9. Optimization of P&R facility location and restriction area under given restriction ratio $\gamma = 0.2$ or $\gamma = 0.5$ (solid orange area: restriction area; dashed lines: restricted road links; solid blue nodes: P&R facility locations)

Table 10. The travel demand, modal-split, and system efficiency metrics under the six solutions in Figure 8

	Solution	TTD	TCF	TPTF	TPRF	AS	PTS	PRS
$\gamma = 0.2$	1	163838.42	95524.71	53594.44	14719.27	58.30%	32.71%	8.98%
	2	163397.00	89468.18	54867.87	19060.95	54.76%	33.58%	11.67%
	3	163298.11	88389.46	55121.68	19786.97	54.13%	33.76%	12.12%
	Solution	TLC	CS	TEC	NCL		T	
	1	566238.30	4100459.25	89270.95	8		6,8,11,17,21,22,24,27	
	2	475207.03	4087713.48	73426.87	6		1,2,7,9,12,13,22,24,27	
	3	440138.01	4069191.12	67464.62	1		2,4,7,12,15,16,22	
$\gamma = 0.5$	Solution	TTD	TCF	TPTF	TPRF	AS	PTS	PRS
	1	161957.90	82341.66	60355.32	19260.93	50.84%	37.27%	11.89%
	2	161321.64	77980.54	62663.58	20677.52	48.34%	38.84%	12.82%
	3	160747.79	73568.84	64553.60	22625.35	45.77%	40.16%	14.08%
	Solution	TLC	CS	TEC	NCL		T	
	1	410780.65	4048947.54	58594.79	5		12,13,14,16,18,19,20,22	
	2	345486.27	4033040.93	45095.89	3		5,10,12,13,14,17,19,21,22	
	3	293343.54	3988300.32	34886.86	0		4,6,10,12,13,14,16,18,22	

5.2 A real example of Eastern Massachusetts highway subnetwork

In this section, we will test the proposed model and algorithm on Eastern Massachusetts highway subnetwork network. The Eastern Massachusetts highway subnetwork network has 110 areas, 74 nodes, 258 links, and 2664 OD pairs, as shown in Figure 10. Detailed network parameters, such as the free flow time, length of each link, link capacity and OD demand can be found in Bar-Gera (2016). Other settings are identical to that in Section 5.1.

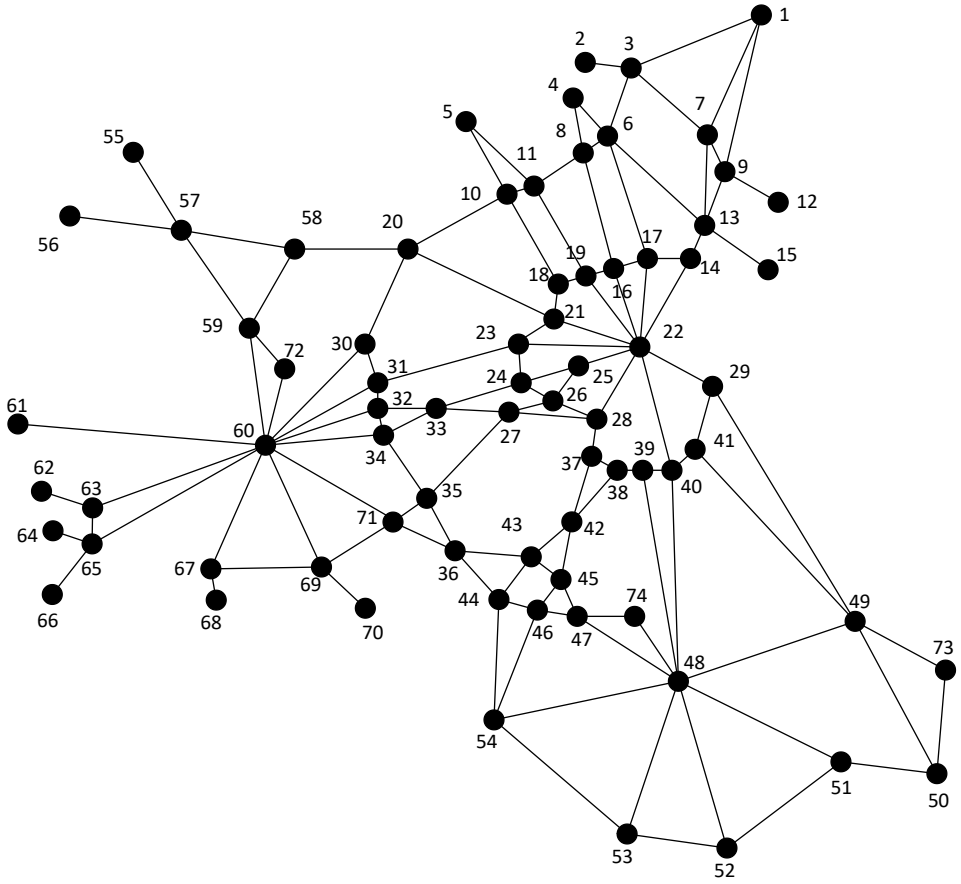

Figure 10. The handled Eastern Massachusetts highway subnetwork network

In the NSGA-II, we set the values of population size and the maximal number of the generation to be 60 and 1000, and the other setting are identical to those in Section 5.1. The total CPU time is 16.2 hours. The solution Pareto frontier (tri-objective) is shown in Figure 11. We also pick up one solution that has a balanced preference over the three objectives, as marked in Figure 11. The optimal P&R facility locations and ATR scheme under this solution are further illustrated in Figure 12, where the solid blue node is the P&R facility location, and the solid orange area and associated lines indicate the restricted areas.

For this Eastern Massachusetts highway subnetwork example, the computation time is 16.2 hours. For super-large networks that are much larger than the current one, they might be aggregated as a more abstract network for the purpose of optimizing P&R facility location and ATR scheme, where the abstract network model can still be solved by the proposed approach in this paper. Alternatively, more efficient heuristics might have to be used and more efficient algorithms for solving the lower-level network equilibrium might have to be developed as well.

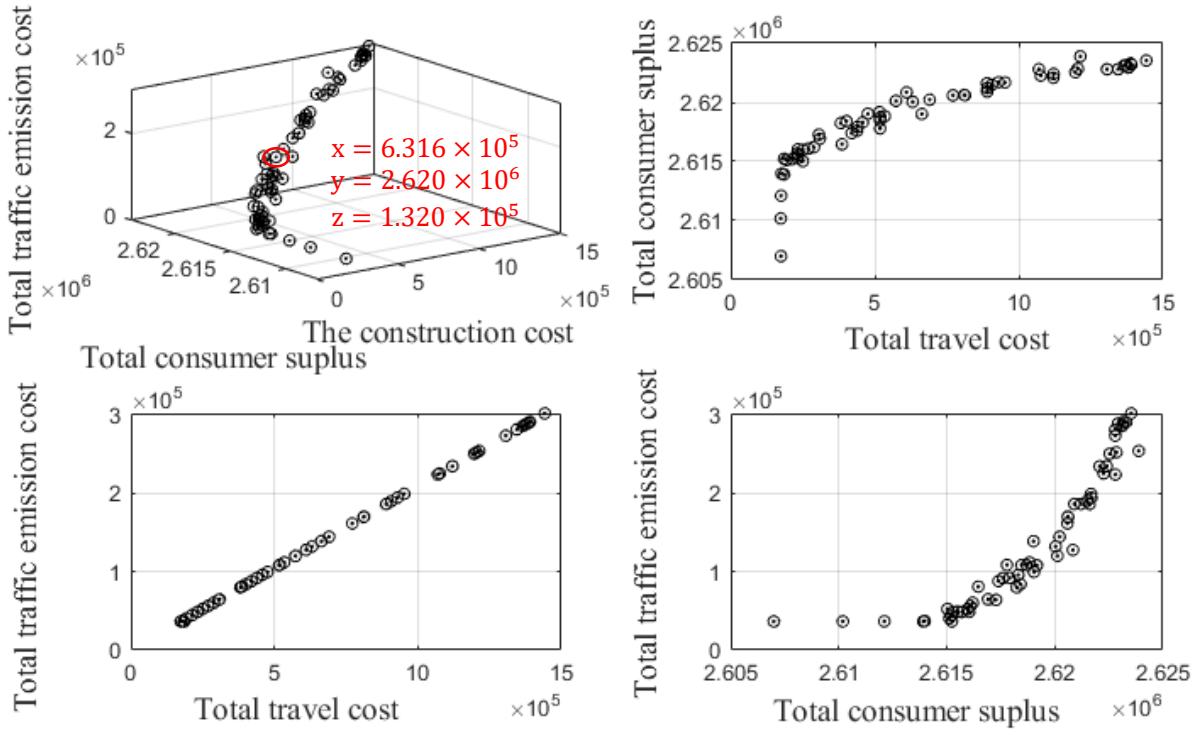

Figure 11. Pareto frontier: joint optimization of P&R facility location and ATR scheme

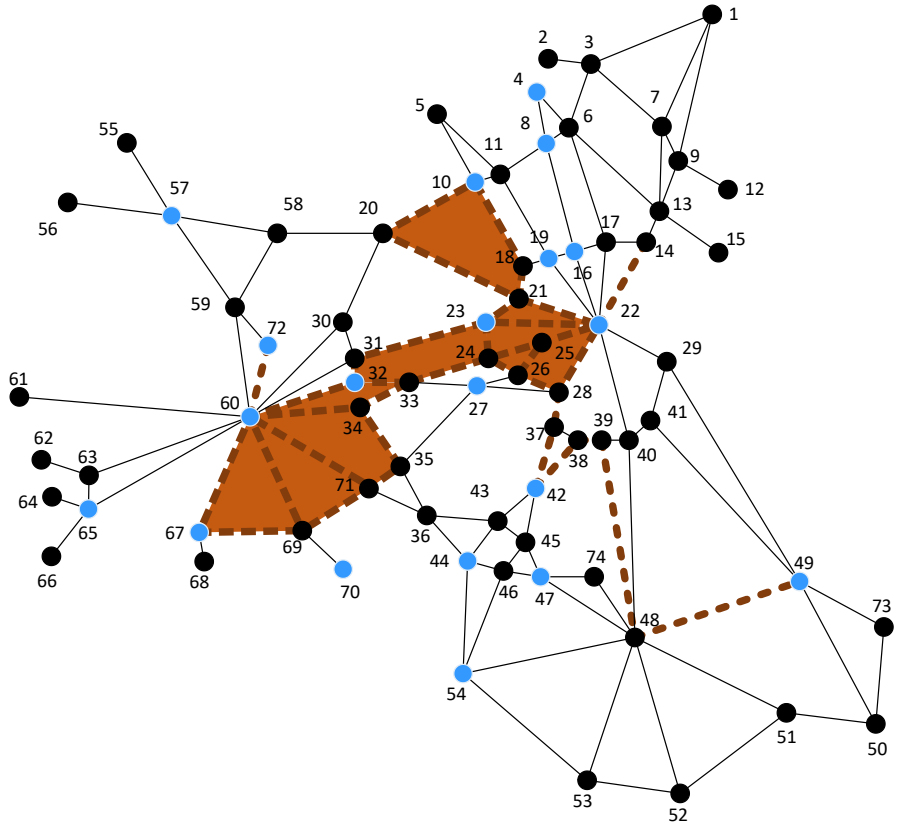

Figure 12. The P&R facility location and ATR scheme of the solution ($\gamma = 0.2381$)

6. Conclusion

This paper develops and presents a multi-objective bi-level model for jointly optimizing P&R facility locations and ATR scheme. The model optimizes the P&R facility location and ATR scheme from three aspects: minimization of user cost, minimization of emission cost, and maximization of consumer surplus, subject to users' mode choices and route choices, which are governed by P&R facility locations and ATR scheme. The NSGA-II algorithm is adapted to solve the tri-objective bi-level model, where the lower-level multimodal network equilibrium problem is solved through a gradient project algorithm. The above three efficiency metrics can be simultaneously considered in the proposed multi-objective framework. Different optimal solutions along the Pareto frontier (for the tri-objective optimization) might be adopted in response to different valuation or preference over the three objectives, as discussed in the numerical studies. This study provides a modeling device for the joint design of P&R facilities and ATR scheme that benefits the users and the society.

In practice, it is possible that the locations of park-and-ride facilities might be determined first without consideration of the alternate traffic restriction (ATR) scheme (Problem 1). With given park-and-ride facilities, the regulator may further design an ATR scheme to manage traffic (Problem 2). The above two problems are indeed special cases under the proposed model. Problem 1 can be formulated with the proposed model by assuming no ATR scheme (zero traffic to be restricted), and Problem 2 can be formulated with the proposed model by assuming given park-and-ride facilities. Instead of solving the above two problems separately, this paper aims to improve system efficiency by jointly optimizing the locations of park-and-ride facilities and the ATR scheme (only applicable when doing the joint optimization is feasible), and illustrates the benefit from such an integrated optimization approach.

This study can be extended along several avenues. Firstly, this paper considers that if park-and-ride facilities are provided at a location, the capacity will be sufficient (larger than the equilibrium flows). This might be the case when park-and-ride is provided at the boundary of city centers or sub-centers (Liu and Geroliminis, 2017). It is of our interest to incorporate rigid parking capacity constraints, such as those in Zhang et al. (2019), Zhang et al., (2020), Liu et al. (2021), and Liu et al. (2022). Then, the lower-level traffic equilibrium will be a capacity-constrained equilibrium problem, and the parking capacity constraints will be associated with potential competition behaviors for limited parking. Secondly, discounted fares on public transport associated with park-and-ride service might be optimized to further improve overall system efficiency and maximize the potential benefits from providing park-and-ride options. A joint optimization model of park-and-ride location, ATR scheme, and public transport fare and discount scheme can be further developed. Thirdly, this paper uses the logit-model for

simplicity to model the modal-split. A future study might utilize different choice models (such as the C-Logit model or Probit-model) to better account for the correlations among different modes. In addition, a future study may examine heuristics other than NSGA-II that might be adapted for super-large network applications.

Acknowledgement

This research was partly supported by grants from the National Natural Science Foundation of China (72171236, 71701216, 71871226), the National Key R&D Program of China (2020YFB1600400), the Natural Science Foundation of Hunan Province (2020JJ5783). Dr. Wei Liu would like to acknowledge the support from The Hong Kong Polytechnic University (P0039246, P0040900, P0041316).

References

Arnott, R., Palma, A. and Lindsey, R., 1991. A temporal and spatial equilibrium analysis of commuter parking. Journal of Public Economics, 45(3), 301-335.

Aros-Vera, F., Marianov, V. and Mitchell, J.E., 2013. P-hub approach for the optimal park-and-ride facility location problem. European Journal of Operational Research, 226(2), 277-285.

Cantarella, G.E., 1997. A general fixed-point approach to multimode multi-user equilibrium assignment with elastic demand. Transportation Science, 31(2), 107-128.

Castillo, E., Calvino, A., Nogal, M. and Lo, H.K., 2014. On the probabilistic and physical consistency of traffic random variables and models. Computer-Aided Civil and Infrastructure Engineering, 29(7), 496-517.

Cheng, Q., Liu, Z. and Szeto, W.Y., 2019. A cell-based dynamic congestion pricing scheme considering travel distance and time delay. Transportmetrica B: Transport Dynamics, 7(1), 1286-1304.

Cipriani, E., Gori, S. and Petrelli, M., 2010. Transit network design: A procedure and an application to a large urban area. Transportation Research Part C: Emerging Technologies, 20(1), 3-14.

Daganzo, C.F., 1995. A Pareto optimum congestion reduction scheme. Transportation Research Part B: Methodological, 29(2),139-154.

Daganzo, C.F. and Garcia, R.C., 2011. A Pareto improving strategy for the time-dependent morning commute problem. Transportation Science, 34 (3), 303-311.

Deb, K., Agrawal, S., Pratap, A. and Meyarivan, T.A., 2002. A fast elitist multi-objective genetic algorithm: NSGA-II. IEEE Transactions on Evolutionary Computation, 6(2), 182-197.

Dijk, M. and Montalvo, C., 2011. Policy frames of park-and-ride in Europe. Journal of Transport Geography, 19(6), 1106-1119.

Duncan, M. and Christensen, R.K., 2013. An analysis of park-and-ride provision at light rail stations across the US. Transport Policy, 25, 148-157.

Farhan, B. and Murray, A.T., 2008. Siting park-and-ride facilities using a multi-objective spatial optimization model. Computers & Operations Research, 35(2), 445-456.

Fernández, J.E., de Cea, J. and Soto, A., 2003. A multi-modal supply-demand equilibrium model for predicting intercity freight flows. Transportation Research Part B: Methodological, 37(7), 615-640.

Fu, X., Lam, W.H.K., Chen, B.Y. and Liu, Z.Y., 2020. Maximizing space-time accessibility in multi-modal transit networks: an activity-based approach. Transportmetrica A: Transport Science, 1-29. DOI: 10.1080/23249935.2020.1806372

Gao, Z., Wu, J. and Sun, H., 2005. Solution algorithm for the bi-level discrete network design problem. Transportation Research Part B: Methodological, 39(6), 479-495.

Grange, L.D. and Troncoso, R., 2011. Impacts of vehicle restrictions on urban transport flows: The case of Santiago, Chile. Transport Policy, 18(6), 862-869.

Han, D., Yang, H. and Wang, X., 2010. Efficiency of the plate-number-based traffic rationing in general networks. Transportation Research Part E: Logistics and Transportation Review, 46(6), 1095-1110.

Han, L., Zhu, C., Wang, D.Z. and Wu, J., 2021. A discrete-time second-best dynamic road pricing scheme considering the existence of multiple equilibria. Transportmetrica B: Transport Dynamics, 9(1), 303-323.

Ho, H.W., Wong S.C. and Loo B.P.Y., 2006. Combined distribution and assignment model for a continuum traffic equilibrium problem with multiple user classes. Transportation Research Part B: Methodological, 40(8), 633-655.

Huang, D., Liu, Z., Fu, X. and Blythe, P.T., 2018. Multimodal transit network design in a hub-and-spoke network framework. Transportmetrica A: Transport Science, 14(8), 706-735.

Huang, W., Xu, G.M. and Lo, H.K., 2020. Pareto-optimal sustainable transportation network design under spatial queuing. Networks & Spatial Economics, 20(3), 637-673.

Jakob, M. and Menendez, M., 2020. Parking pricing vs. congestion pricing: a macroscopic analysis of their impact on traffic. Transportmetrica A: Transport Science, 17(4), 462-491.

Lindsey, R., 2010. Reforming road user charges: a research challenge for regional science. Journal of Regional Science, 50(1), 471-492.

Liu, T., Ceder, A. and Chowdhury., 2017. Integrated public transport timetable synchronization with vehicle scheduling. Transportmetrica A: Transport Science, 13 (10), 932-954.

Liu, T.L., Huang, H.J., Yang, H. and Zhang, X., 2009. Continuum modeling of park-and-ride services in a linear monocentric city with deterministic mode choice. Transportation Research Part B: Methodological, 43(6), 692-707.

Liu, W. and Geroliminis, N., 2016. Modeling the morning commute for urban networks with cruising-for-parking: An MFD approach. Transportation Research Part B: Methodological, 93, 470-494.

Liu, W. and Geroliminis, N., 2017. Doubly dynamics for multi-modal networks with park-and-ride and adaptive pricing. Transportation Research Part B: Methodological, 102, 162-179.

Liu, W., Yang, H. and Yin, Y.F., 2014. Traffic rationing and pricing in a linear monocentric city. Journal of Advanced Transportation, 48(6), 655-672.

Liu, W., Zhang, F., Wang, X., Shao, C. and Yang, H., 2022. Unlock the Sharing Economy: The Case of the Parking Sector for Recurrent Commuting Trips. Transportation Science, 1-20. DOI: 10.1287/trsc.2021.1103

Liu, W., Zhang, F. and Yang, H., 2021. Modeling and managing the joint equilibrium of destination and parking choices under hybrid supply of curbside and shared parking. Transportation Research Part C: Emerging Technologies, 130, 103301.

Liu, Z., Chen, X., Meng, Q. and Kim, I., 2018. Remote park-and-ride network equilibrium model and its applications. Transportation Research Part B: Methodological, 117, 37-62.

Liu, Z. and Meng, Q., 2014. Bus-based park-and-ride system: a stochastic model on multimodal network with congestion pricing schemes. International Journal of Systems Science, 45(5), 994-1006.

Mankiw, N.G., 2003. Principles of economics. South-Western College Pub.

Nakamura, K. and Kockelman, K., 2002. Congestion pricing and road space rationing: an application to the San Francisco Bay bridge corridor. Transportation Research Part A: Policy and Practice, 36(5), 403-417.

Nie, Y.M., 2017. On the potential remedies for license plate rationing. Economics of Transportation, 9, 37-50.

Penic, M.A. and Upchurch, J., 1992. TRANSYT-7F: enhancement for fuel consumption, pollution emissions, and user costs. Transportation Research Record, 1360, 104-111.

Pineda, C., Cortés, C.E., Jara-Moroni, P. and Moreno, E., 2016. Integrated traffic-transit stochastic equilibrium model with park-and-ride facilities. Transportation Research Part C: Emerging Technologies, 71, 86-107.

Shi, F., Xu, G., Liu, B. and Huang, H., 2014. Optimization method of alternate traffic restriction scheme based on elastic demand and mode choice behavior. Transportation Research Part C: Emerging Technologies, 39(2), 36-52.

Song, Z., He, Y. and Zhang, L., 2017. Integrated planning of park-and-ride facilities and transit service. Transportation Research Part C: Emerging Technologies, 74, 182-195.

Song, Z., Yin, Y., Lawphongpanich, S. and Yang, H., 2013, A Pareto-improving hybrid policy for transportation networks. Journal of Advanced Transportation, 48(3), 272-286.

Tran, C.Q., Ngoduy, D., Keyvan-Ekbatani M. and Watling, D., 2020. A user equilibrium-based fast-charging location model considering heterogeneous vehicles in urban networks. Transportmetrica A: Transport Science, 17 (4), 439-461.

Wang, J.Y., Yang, H. and Lindsey, R., 2004. Locating and pricing park-and-ride facilities in a linear monocentric city with deterministic mode choice. Transportation Research Part B: Methodological, 38(8), 709-731.

Wang, X.L., Yang, H., Zhu, D.L. and Li, C.M., 2012. Tradable travel credits for congestion management with heterogeneous users. Transportation Research Part E: Logistics and Transportation Review, 48 (2), 426-437.

Wong, S.C., Wong, C.K. and Tong, C.O., 2001. A parallelized genetic algorithm for the calibration of Lowry model. Parallel Computing, 27(12), 1523-1536.

Wu, D., Yin Y., Lawphongpanich, S. and Yang, H., 2012. Design of more equitable congestion pricing and tradable credit schemes for multimodal transportation networks. Transportation Research Part B: Methodological, 46(9), 1273-1287.

Yang, H. and Bell, M.G., 1998. Models and algorithms for road network design: a review and some new developments. Transport Reviews, 18(3), 257-278.

Yang, H. and Huang, H.J., 2005. Mathematical and Economic Theory of Road Pricing. Emerald Group Publishing Limited 2005.

Yang, H. and Wang, X.L., 2011. Managing network mobility with tradable credits. Transportation Research Part B: Methodological, 45(3), 580-594.

Zhang, F., Liu, W., Wang, X. and Yang, H., 2020. Parking sharing problem with spatially distributed parking supplies. Transportation Research Part C: Emerging Technologies, 117, 102676.

Zhang, X., Liu, W. and Waller, S.T., 2019. A network traffic assignment model for autonomous vehicles with parking choices. Computer-Aided Civil and Infrastructure Engineering, 34(12), 1100-1118.

Zhang, X.N., Huang, H.J. and Zhang, H.M., 2008. Integrated daily commuting patterns and optimal road tolls and parking fees in a linear city. Transportation Research Part B: Methodological, 42(1), 38-56.

Zhang, X.N. and Yang, H., 2004. The optimal cordon-based network congestion pricing problem. Transportation Research Part B: Methodological, 38(6), 517-537.